

ACCEPTED MANUSCRIPT • OPEN ACCESS

## Future climate change significantly alters interannual wheat yield variability over half of harvested areas

To cite this article before publication: Weihang Liu *et al* 2021 *Environ. Res. Lett.* in press <https://doi.org/10.1088/1748-9326/ac1fbb>

### Manuscript version: Accepted Manuscript

Accepted Manuscript is “the version of the article accepted for publication including all changes made as a result of the peer review process, and which may also include the addition to the article by IOP Publishing of a header, an article ID, a cover sheet and/or an ‘Accepted Manuscript’ watermark, but excluding any other editing, typesetting or other changes made by IOP Publishing and/or its licensors”

This Accepted Manuscript is © 2021 The Author(s). Published by IOP Publishing Ltd.

As the Version of Record of this article is going to be / has been published on a gold open access basis under a CC BY 3.0 licence, this Accepted Manuscript is available for reuse under a CC BY 3.0 licence immediately.

Everyone is permitted to use all or part of the original content in this article, provided that they adhere to all the terms of the licence <https://creativecommons.org/licenses/by/3.0>

Although reasonable endeavours have been taken to obtain all necessary permissions from third parties to include their copyrighted content within this article, their full citation and copyright line may not be present in this Accepted Manuscript version. Before using any content from this article, please refer to the Version of Record on IOPscience once published for full citation and copyright details, as permissions may be required. All third party content is fully copyright protected and is not published on a gold open access basis under a CC BY licence, unless that is specifically stated in the figure caption in the Version of Record.

View the [article online](#) for updates and enhancements.

1  
2  
3  
4 **1 Future climate change significantly alters interannual wheat yield**  
5  
6 **2 variability over half of harvested areas**

7  
8 **3 Authors:** Weihang Liu<sup>1,2,3</sup>, Tao Ye<sup>1,2,3,4</sup>, Jonas Jägermeyr<sup>5,6,7</sup>, Christoph Müller<sup>7</sup>, Shuo  
9  
10 **4** Chen<sup>1,2,3</sup>, Xiaoyan Liu<sup>1,2,3</sup> and Peijun Shi<sup>1,2,3,8</sup>

11  
12 <sup>1</sup>Academy of Disaster Reduction and Emergency Management, Faculty of Geographical Science,  
13  
14 Beijing Normal University, Beijing 100875, China

15  
16 <sup>2</sup>Key Laboratory of Environmental Change and Natural Disaster, Ministry of Education, Faculty of  
17  
18 Geographical Science, Beijing Normal University, Beijing 100875, China

19  
20 <sup>3</sup>State Key Laboratory of Earth Surface Processes and Resource Ecology, Faculty of Geographical  
21  
22 Science, Beijing Normal University, Beijing 100875, China

23  
24 <sup>4</sup>The Frederick S. Pardee Center for the Study of the Longer-Range Future and Department of Earth  
25  
26 and Environment, Boston University, Boston, MA 02215, USA

27  
28 <sup>5</sup>NASA Goddard Institute for Space Studies, New York, NY 10025, USA

29  
30 <sup>6</sup>Center for Climate Systems Research, Columbia University, New York, NY 10025, USA

31  
32 <sup>7</sup>Potsdam Institute for Climate Impact Research (PIK), Member of the Leibniz Association, 14412,  
33  
34 Potsdam, Germany

35  
36 <sup>8</sup>Academy of Plateau Science and Sustainability, People's Government of Qinghai Province and  
37  
38 Beijing Normal University, Xining 810016, China

39  
40 Author for correspondence: Tao Ye ([yetao@bnu.edu.cn](mailto:yetao@bnu.edu.cn))

41  
42 Room B931, Jingshikeji Building, Beijing Normal University

43  
44 No. 12 Xueyuannan Rd., Haidian District

45  
46 Beijing 100082, China

47  
48 Tel/fax: +86-10-58800268

49  
50 Tel: +86-10-58800268, ORCID: 0000-0002-5037-8410

51  
52  
53  
54  
55  
56  
57  
58  
59  
60

1  
2  
3  
4 28 **Future climate change significantly alters interannual wheat yield**  
5  
6 29 **variability over half of harvested areas**  
7  
8  
9

10 30 **Abstract**  
11  
12

13  
14 31 Climate change affects the spatial and temporal distribution of crop yields, which can  
15 32 critically impair food security across scales. A number of previous studies have  
16 33 assessed the impact of climate change on mean crop yield and future food availability,  
17 34 but much less is known about potential future changes in interannual yield variability.  
18  
19 35 Here, we evaluate future changes in relative interannual global wheat yield variability  
20 36 (the coefficient of variation; CV) at 0.25° spatial resolution for two representative  
21 37 concentration pathways (RCP4.5 and RCP8.5). A multi-model ensemble of crop model  
22 38 emulators based on global process-based models is used to evaluate responses to  
23 39 changes in temperature, precipitation, and CO<sub>2</sub>. The results indicate that over 60% of  
24 40 harvested areas could experience significant changes in interannual yield variability  
25 41 under a high-emission scenario by the end of the 21<sup>st</sup> century (2066–2095). 31% and  
26 42 44% of harvested areas are projected to undergo significant reductions of relative yield  
27 43 variability under RCP4.5 and RCP8.5, respectively. In turn, wheat yield is projected to  
28 44 become more unstable across 23% (RCP4.5) and 18% (RCP8.5) of global harvested  
29 45 areas—mostly in hot or low fertilizer input regions, including some of the major  
30 46 breadbasket countries. The major driver of increasing yield CV change is the increase  
31 47 in yield standard deviation, whereas declining yield CV is mostly caused by stronger  
32 48 increases in mean yield than in the standard deviation. Changes in temperature are the  
33 49 dominant cause of change in wheat yield CVs, having a greater influence than changes  
34 50 in precipitation in 53% and 72% of global harvested areas by the end of the century  
35 51 under RCP4.5 and RCP8.5, respectively. This research highlights the potential  
36 52 challenges posed by increased yield variability and the need for tailored regional  
37 53 adaptation strategies.  
38  
39  
40  
41  
42  
43  
44  
45  
46  
47  
48  
49  
50  
51  
52  
53  
54  
55  
56  
57  
58  
59  
60

1  
2  
3  
4  
54

55 **Keywords:** yield coefficient-of-variation; crop model emulator; contributions of  
6 climatic drivers; yield stability; global food security  
7  
8  
9

## 10 1. Introduction

11  
12  
13

14 Interannual crop yield variability is one of the primary drivers of food system instability  
15 (IPCC 2019). Assessing the effects of climate change on yield variability is critical to  
16 understanding the impact of climate change on food security (FAO, 2019). Due to  
17 trends in global warming (Lobell *et al.*, 2011) and the changing frequency and intensity  
18 of climate extremes (Trnka *et al.*, 2014), potential decreases in the mean yields of crops  
19 and an increase in the interannual yield variability could adversely affect the livelihoods  
20 of producers, create spikes in food prices, lead to hunger (IPCC, 2014), and even cause  
21 political instabilities at a regional level (Sternberg, 2011). Previously, the impact of  
22 climate change on mean crop yield (Rosenzweig *et al.* 2014, Lobell *et al.* 2011) has been  
23 investigated with a focus on food availability (Wollenberg *et al.*, 2016). From a climate  
24 risk perspective, the concept of time of climate impact emergence has recently been  
25 introduced, linking mean yield changes with historical yield variability (Jägermeyr *et*  
26 *al.* 2021). Yet, the impact of climate change on future interannual yield variability has  
27 not received sufficient attention (Wheeler *et al.*, 2013; Challinor *et al.*, 2014).  
28  
29  
30  
31  
32  
33  
34  
35  
36  
37  
38  
39  
40  
41

72

73 Interannual yield variability has always been one of the key risk indicators of crop  
74 production. Early studies have either assumed a stationary process without considering  
75 variability changes (Ray *et al.*, 2015; Tao *et al.*, 2016; Matiu *et al.*, 2017; Ceglar *et al.*,  
76 2016) or linked changes in variability to non-climatic factors (Döring and Reckling  
77 2018, Knapp and van der Heijden 2018, Kucharik and Ramankutty 2005, Müller *et al.*  
78 2018). Recent studies have provided evidence for changes in the interannual yield  
79 variability of major cereal crops and identified significant impacts of climate change at  
80 the global scale 0.5° grid level or at the country level (Osborne and Wheeler, 2013;  
56  
57  
58  
59  
60

1  
2  
3 81 Iizumi and Ramankutty 2016). These studies have been followed up by regional,  
4  
5 82 county-level analyses of the interannual yield variability of maize (Leng, 2017;  
6  
7 83 Hawkins *et al.*, 2013; Lobell *et al.*, 2014). Efforts have also been devoted to projecting  
8  
9 84 the impact of future climate change on interannual yield variability, focusing on wheat  
10  
11 85 and maize at global and regional scales, using process-based crop models (Liu *et al.*,  
12  
13 86 2019; Moriondo *et al.*, 2011) and statistical models (Urban *et al.*, 2012; Ben-Ari *et al.*,  
14  
15 87 2018 Tigchelaar *et al.*, 2018). Results from these studies have indicated substantial  
16  
17 88 changes in interannual yield variability as a result of climate change, and that the sign  
18  
19 89 and magnitude of change varies by production region.  
20

21  
22 91 Climate-related risk assessment on crop yield requires reflecting the spatial  
23  
24 92 heterogeneity of both agricultural systems and climate change effects relevant for  
25  
26 93 interannual yield variability (Benami *et al.*, 2021). There are still major research gaps  
27  
28 94 in our understanding of these linkages across regions. In terms of major staple crops,  
29  
30 95 only changes in yield CV of wheat (Liu *et al.*, 2019) and maize have been analysed  
31  
32 96 (Tigchelaar *et al.*, 2018) at the global scale. As these studies have used either site-based  
33  
34 97 simulation or globally homogeneous warming perturbations, it is difficult to deduce  
35  
36 98 robust conclusions on changes in interannual yield variability, reflecting the spatial  
37  
38 99 heterogeneity of climate projections (Leng and Hall, 2020). In addition, although the  
39  
40 100 mechanism of impact and the mean yield response to change in climate drivers (e.g.,  
41  
42 101 temperature, precipitation, and CO<sub>2</sub>) have been intensively discussed (Zhu *et al.*, 2019;  
43  
44 102 Schlenker and Roberts, 2009), the response of interannual yield variability to changes  
45  
46 103 in the various climate drivers is not well understood.

47  
48 105 The aim of this study is to evaluate potential changes in interannual wheat yield  
49  
50 106 variability under two climate change scenarios globally, and to attribute individual  
51  
52 107 contributions of temperature, precipitation, and CO<sub>2</sub>. The main research questions are:  
53  
54 108 1) How could climate change affect interannual wheat yield variability on current  
55  
56 109 wheat-growing areas by the end of the century? 2) How much of these changes can be

1  
2  
3 110 attributed to changes in temperature, precipitation, and their interaction, respectively?  
4

5 111 3) To what extent can elevated CO<sub>2</sub> concentrations mitigate potential increases in yield  
6  
7 112 variability? Answers to these questions will provide crucial information for climate risk  
8  
9 113 assessment and effective adaptation measures.

10  
11 114

12 115 We address these questions by conducting multi-model ensemble simulations with crop  
13  
14 116 model emulators forced with global climate projections at high spatial resolution  
15  
16 117 (0.25°). Statistical crop model emulators are developed based on simulations from  
17  
18 118 global gridded crop models (GGCMs), facilitated by AgMIP's Global Gridded Crop  
19  
20 119 Model Intercomparison Project (GGCMI). Crop model emulators have recently gained  
21  
22 120 popularity as a powerful tool for assessing the impact of climate change on crop yield  
23  
24 121 (Oyebamiji *et al* 2015, Lobell and Burke 2010, Holzkämper *et al* 2012, Raimondo *et al*  
25  
26 122 2020, Müller *et al* 2021). Emulators substantially improve computational efficiency  
27  
28 123 and reduce data-processing requirements compared to running the original models,  
29  
30 124 without sacrificing much prediction performance (Folberth *et al* 2019, Blanc and Sultan  
31  
32 125 2015, Blanc 2017, Franke *et al* 2020a, Ringeval *et al* 2020). The use of a large ensemble  
33  
34 126 of GCM projections in combination with the ensemble of crop yield emulators allows  
35  
36 127 for comprehensively evaluating changes in future yield variability and the associated  
37  
38 128 distribution of extreme yield levels.

## 39 40 129 **2. Materials and methods**

### 41 42 43 44 130 **2.1 Input data**

#### 45 46 47 131 **2.1.1 Gridded crop model data for emulator construction**

48  
49  
50 132 The input and output data for the simulation of global gridded wheat yield were  
51  
52 133 obtained from the GGCMI phase 2 experiment dataset (Franke *et al.*, 2020b). The  
53  
54 134 spatial resolution of this dataset is 0.5°. The input data included four different data types,  
55  
56 135 i.e., climate, soil, atmospheric CO<sub>2</sub> concentration, and nitrogen fertilizer application

1  
2  
3 136 rates (Table S1, Franke *et al.*, 2020b). Baseline climate inputs were used from the  
4  
5 137 AgMIP Modern-Era Retrospective Analysis for Research and Applications  
6  
7 138 (AgMERRA) forcing dataset (1980-2010), including daily maximum and minimum  
8  
9 139 temperatures, precipitation, and solar radiation (Ruane *et al* 2015). Based on these  
10  
11 140 baseline reference simulations, the GGCM phase 2 experiment used systematic  
12  
13 141 perturbations in each grid cell with seven temperature levels (from -1 K to +6 K in 1K  
14  
15 142 interval, with +5K skipped), nine precipitation levels (from -50% to +30%, in 10%  
16  
17 143 interval, with -40% skipped), four CO<sub>2</sub>-concentration levels (360, 510, 660, and 810  
18  
19 144 ppm), and three nitrogen levels (10, 60, and 200 kg/ha) (Table S2; Franke et al. 2020b).  
20  
21 145 Twelve GGCMs were then forced with each of these perturbations of the original  
22  
23 146 reanalysis weather data. The GGCMs used a national and subnational crop calendar for  
24  
25 147 wheat that is based on Sacks et al (2010), Portmann *et al* (2010), and environment-  
26  
27 148 based extrapolations (Elliott *et al* 2015).

28  
29 150 The output data contained irrigated and rainfed yield simulations from 1980 to 2010 for  
30  
31 151 each of the different perturbation levels. In this study, we selected 8 out of the 12 crop  
32  
33 152 models in the GGCM phase 2 experiment for constructing the emulators. These were  
34  
35 153 APSIM-UGOE, EPIC-IIASA, EPIC-TAMU, GEPIC, LPJ-GUESS, LPJmL, pDSSAT,  
36  
37 154 and PEPIC. CARAIB was not included as it did not consider nitrogen stress.  
38  
39 155 ORCHIDEE-crop was not included as it did not provide simulation results for spring  
40  
41 156 wheat. PROMET and JULES were not included as they used different climate inputs.  
42  
43 157 Although these eight crop models differed in their representation of crop phenology,  
44  
45 158 leaf-area development, yield formation, root expansion, and nutrient assimilation, all  
46  
47 159 accounted for the effects of water and heat stress and assumed no technological change  
48  
49 160 (Blanc, 2017). All input and output data sets were provided by GGCM at the  
50  
51 161 standardized spatial resolution of 0.5°. More detailed descriptions of the individual crop  
52  
53 162 models and the input and output data characteristics are available in the Supplementary  
54  
55 163 Material (SM).

### 164 **2.1.2 Data for emulator-based yield projections**

165 To project a high spatial resolution global wheat yield, the Earth Exchange Global Daily  
166 Downscaled Projections (NEX-GDDP) dataset (Thrasher 2012), with a spatial  
167 resolution of 0.25°, was obtained from the National Aeronautics Space Administration  
168 (NASA). This database contains the global daily maximum/minimum near-surface air  
169 temperature and precipitation data from 21 GCMs from the Coupled Model  
170 Intercomparison Project phase 5 (CMIP5, Taylor *et al* 2012) under two representative  
171 concentration pathways (RCP4.5 and RCP8.5), covering the years 1950–2100. Other  
172 RCPs are not available through NEX-GDDP.

173

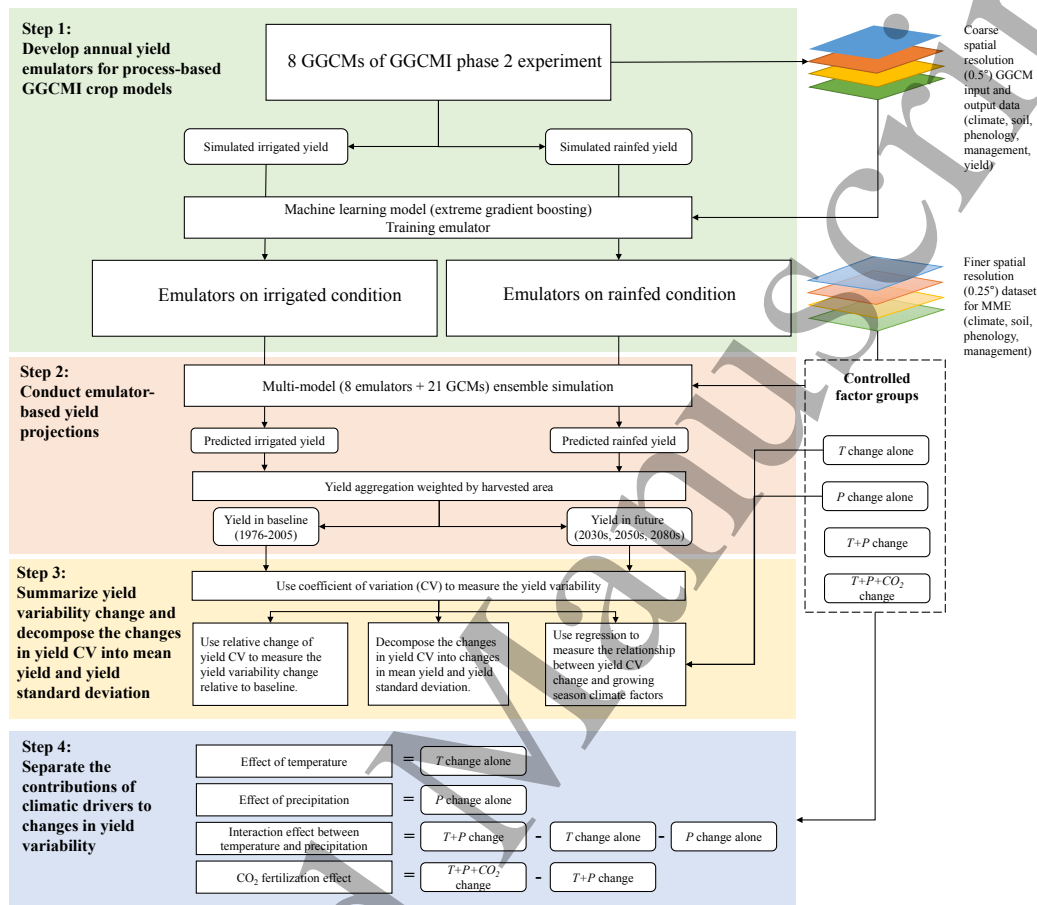
174 The emulator-based projections used a national and subnational crop calendar for wheat  
175 from MIRCA2000 (Portmann *et al* 2010). Given that MIRCA2000 has only monthly  
176 resolution, it was assumed that the first day of the month was the date of planting, and  
177 the last day of the month was the date of harvesting (Elliott *et al* 2015). The calendar  
178 we used to project yield was only MIRCA2000 because if we used the calendar of the  
179 GGCM phase 2, we would be troubled with the mismatch between the separated spring  
180 and winter wheat calendar and only wheat harvested areas in SPAM. Global wheat  
181 harvested area distribution around the year 2005 was obtained from the spatial  
182 production allocation model (SPAM) for rainfed and irrigated systems at five arc-  
183 minute resolution (You *et al* 2014).

### 184 **2.2 Methods**

185 The methodologies for evaluating changes in wheat yield variability under future  
186 climate scenarios includes the following steps (Figure 1): 1) Develop annual yield  
187 emulators for the process-based GGCM crop models. 2) Conduct emulator-based  
188 yield projections based on the NEX-GDDP climate model ensemble. 3) Summarize the  
189 future changes in wheat yield variability relative to the baseline; decompose the  
190 changes in yield variability into changes in mean yield and yield standard deviation.



191 And 4) Separate the contributions from the changes in climatic drivers to the changes  
 192 in the yield variability.



193  
 194 **Figure 1** Framework for evaluating changes in global wheat yield interannual variability ( $T$ : temperature,  
 195  $P$ : precipitation).

### 196 2.2.1 Development of annual GGCM emulators by extreme gradient boosting

197 A previous study developed emulators of climatological-mean yield based on GGCM  
 198 phase 2 experiment data (Franke *et al.*, 2020a). We, however, develop an emulator  
 199 capable of capturing year-to-year variability in yield. A machine-learning approach was  
 200 used in this study for its flexibility for data-driven development of models with high  
 201 accuracy (Folberth *et al.*, 2019) and its associated computational efficiency.

202  
 203 Development of the emulator consists of training—via a machine-learning (ML)  
 204 algorithm—on specific GGCM input and output datasets, so that the emulator replicates

1  
2  
3 205 the complex process of yield simulation within the crop model. Variables that have  
4  
5 206 been frequently reported to significantly influence wheat yield were prepared as the  
6  
7 207 predicting variables, including climate, soil type, length of growing season, and  
8  
9 208 management practices (Table S3). All the data for training were computed/adapted  
10  
11 209 from the GGCMs' input and output datasets.

12  
13 210

14 211 All prediction variables were computed/obtained from the GGCM phase 2 data archive.  
15  
16 212 The climate data are supplied as daily values and were, in a first step, aggregated to  
17  
18 213 monthly sums or averages (MON). For each grid, the month of planting was defined as  
19  
20 214 month 1 to harmonize, on a global basis, the order of months from planting.  
21  
22 215 Subsequently, prediction variables were calculated for each month in the growing-  
23  
24 216 season months and the entire growing season (GS, based on the planting and harvesting  
25  
26 217 dates for the GGCMs). Soil properties were adopted primarily for the topsoil class.  
27  
28 218 Additional characteristics like length of growing season were regarded as a cultivar  
29  
30 219 characteristic. The total amount and fraction of the nitrogen fertilizer application and  
31  
32 220 CO<sub>2</sub> concentration were uniform for each grid.

33 221

34 222 In total, 32 different emulators were trained for the eight GGCMs, each with two water  
35  
36 223 management modalities (rainfed and irrigation) and two wheat types (spring wheat and  
37  
38 224 winter wheat). An extreme gradient boosting (XGB) algorithm was used due to its  
39  
40 225 better performance in terms of goodness-of-fit, cross-validation errors, and  
41  
42 226 computation efficiency compared with a random forest algorithm (Folberth *et al.*, 2019).  
43  
44 227 The predicting variables and the simulated yield in the GGCMs were randomly split  
45  
46 228 into training and validation sets, which contained 75% and 25% of the samples (Yue *et*  
47  
48 229 *al.*, 2019), respectively. Depending on the size of the dataset supplied by each GGCM,  
49  
50 230  $1.7 \times 10^6$ – $2.3 \times 10^7$  ( $0.9 \times 10^7$ – $1.9 \times 10^8$ ) samples were used for model training and  $0.6 \times$   
51  
52 231  $10^6$ – $0.8 \times 10^7$  ( $0.3 \times 10^7$ – $0.6 \times 10^8$ ) samples were used for validation of irrigation (rainfed)  
53  
54 232 conditions, covering the period of 1981–2010. More details on emulator training,  
55  
56 233 validation, and performance evaluation are available in SM and Figures S1 and S2.

### 234 **2.2.2 Emulator-based wheat yield projections**

235 The emulators were then used to project global wheat yield by using future GCM  
236 projections. It is important to ensure that emulator-based projections do not exceed the  
237 range of training samples to avoid unrealistic extrapolation effects (Franke *et al* 2020a,  
238 Folberth *et al* 2019). The GGCM phase 2 perturbations were designed to accommodate  
239 high-end warming scenarios (RCP8.5-2080s). For growing season average maximum  
240 temperature, the range of training data (interannual and spatial variability in  
241 AgMERRA + GGCM perturbation) covered the entire range of the GCM projections.  
242 CO<sub>2</sub> concentrations were averaged with a 30-year moving window and the highest CO<sub>2</sub>  
243 concentration under RCP8.5-2080s is 760 ppm.

244

245 Ensemble yield projections were conducted at the global level for grids with a spatial  
246 resolution of 0.25° for the years 1976–2005 (baseline), 2006–2035 (2030s), 2036–2065  
247 (2050s), and 2066–2095 (2080s) under RCPs of 4.5 and 8.5. If the spring and winter  
248 wheat are grown in parallel at national or subnational level, we determined the wheat  
249 type with larger harvested areas according to MIRCA2000 (Portmann *et al.* 2010). The  
250 multi-model ensemble approach improves the robustness of future climate-change  
251 impact estimates and allows for analyses of spatial heterogeneity and inter-model  
252 uncertainty (Martre *et al.*, 2015). There were 336 future wheat yield estimates (21  
253 GCMs × 8 emulators × 2 RCPs), each simulated for 4 × 30-year periods. Throughout  
254 all simulations, planting dates, cultivar selection, soil properties, and management  
255 practices were assumed to remain constant over time, which is consistent with the  
256 GGCM Phase 2 experimental design A0 (Franke *et al* 2020b), which is used for  
257 training the emulators here. Final estimates of future yield responses are based on the  
258 median across the crop model emulators and GCMs.

### 259 **2.2.3 Measuring the change in yield variability**

260 Rainfed and irrigated yield were first aggregated to grid and national levels using an

261 area-weighted average (Müller *et al* 2017), as described in the following equation:

$$262 \quad y_t = \frac{\sum_{i=1}^n y_{i, \text{firr}, t} \times \text{area}_{\text{firr}} + \sum_{i=1}^n y_{i, \text{noirr}, t} \times \text{area}_{\text{noirr}}}{\sum_{i=1}^n (\text{area}_{\text{firr}} + \text{area}_{\text{noirr}})} \quad (1)$$

263 where  $i$  is the index of any grid cell assigned to the spatial unit in year  $t$ ,  $n$  is the number  
 264 of grid cells in that spatial unit,  $y_{i, \text{firr}, t}$  is the emulator-projected yield under fully  
 265 irrigated conditions in grid cell  $i$ , and  $y_{i, \text{noirr}, t}$  is the emulator-projected yield for  
 266 rainfed conditions in grid cell  $i$ ;  $\text{area}$  is the harvested area in grid cell  $i$ , either due to  
 267 fully irrigated or rainfed, obtained from SPAM.

268  
 269 We used the coefficient of variation (CV) a measure of interannual yield variability,  
 270 where  $CV = s/m$ , in which  $s$  and  $m$  are the standard deviation and mean,  
 271 respectively, over a reference period. We compare the baseline period (1976-2005) with  
 272 six future scenario-periods: RCP4.5-2030s, RCP4.5-2050s, RCP4.5-2080s, RCP8.5-  
 273 2030s, RCP8.5-2050s, and RCP8.5-2080s. The percentage change in yield CV in one  
 274 of the six future scenario-periods relative to the baseline period is then measured by:

$$275 \quad d_{\text{scenario}} = \frac{CV_{\text{scenario}} - CV_{\text{baseline}}}{CV_{\text{baseline}}} \times 100\% \quad (2)$$

276

#### 277 **2.2.4 The effects of changes in temperature, precipitation, and CO<sub>2</sub>**

278 The effects of changes in temperature, precipitation, and CO<sub>2</sub> were separated by using  
 279 individual climate driver perturbed simulations, with one climate factor at a time taken  
 280 from a climate scenario and the rest from the baseline. Four such climate driver  
 281 sensitivity simulations (Table 1) were conducted to isolate the effects of changes in  
 282 temperature, precipitation, their interaction effects, and the CO<sub>2</sub> fertilization effect.

283 **Table 1** Climate driver sensitivity simulations

284 Climate drivers	285 Descriptions
---------------------	------------------

“T”	Using future scenarios of temperature, other drivers taken from baseline
“P”	Using future scenarios of precipitation, other drivers taken from baseline
“T+P”	Using future scenarios of temperature and precipitation, holding CO <sub>2</sub> constant at 360 ppm
“T+P+CO <sub>2</sub> ”	Using future scenarios of temperature, precipitation, and CO <sub>2</sub>

284 The climate driver sensitivity simulations listed in Table 1 allow for addressing the  
285 following:

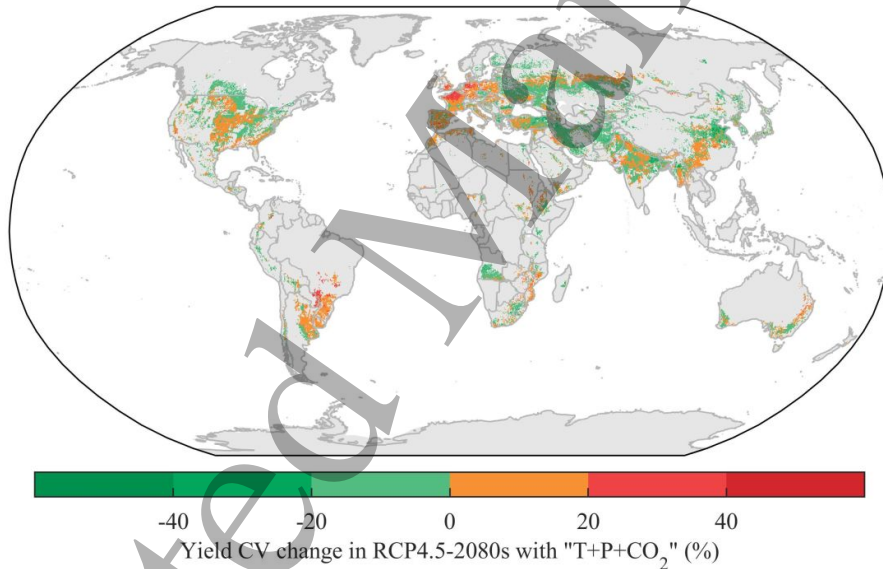
- 286 1) The effects of temperature and precipitation changes can be derived by comparing  
287 the results of groups “T” and “P” with the baseline simulations, respectively.
- 288 2) The interaction between temperature and precipitation changes can be evaluated  
289 using the difference between groups “T+P” and “T” + “P”.
- 290 3) The effect of CO<sub>2</sub> fertilization can be evaluated using the difference between groups,  
291 “T+P+CO<sub>2</sub>” and “T+P”.

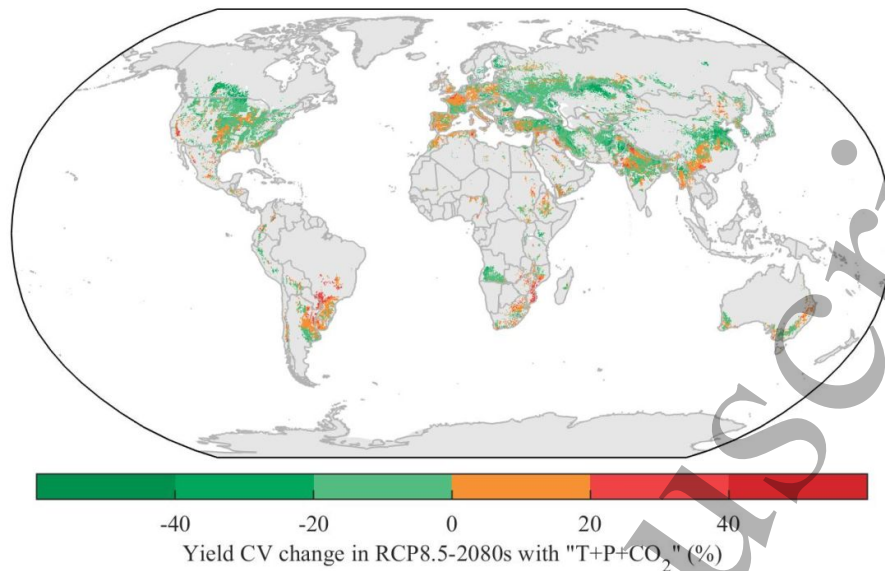
### 292 3. Results

#### 293 3.1 Global patterns of future change in wheat yield interannual variability

294 By the end of the century, model simulations indicate an overall decrease in wheat yield  
295 CV, but in some regions, including major producing countries, there would be more  
296 unstable wheat yield (Figure 2). The spatial patterns of CV changes intensify towards  
297 the end of the century, indicating a more polarized pattern under the long-term scenarios  
298 RCP4.5-2080s and RCP8.5-2080s (Figure S3). Under RCP8.5-2080s, with the CO<sub>2</sub>  
299 fertilization effect (“T+P+CO<sub>2</sub>”), the yield CV increases significantly in 18% of  
300 harvested areas ( $p < 0.05$ ; see Figure S4 for significance test), while 44% of harvested  
301 areas experience significant decrease of the yield CV ( $p < 0.05$ ). Under RCP4.5-2080s,  
302 with the CO<sub>2</sub> fertilization effect (“T+P+CO<sub>2</sub>”), 23% of harvested areas undergoes  
303 significant increase of yield CV ( $p < 0.05$ ), while yield becomes more stable in 31% of  
304 harvested areas significantly ( $p < 0.05$ ). Western Europe, northern Australia, central US,  
305 South Asia, Southwest China, and Myanmar are found to experience a small increase

1  
2  
3 306 in yield CV (<40%). In eastern Europe, southern Australia, and central India yield CV  
4 307 is indicated to decrease by >20% under RCP8.5-2080s (Figure 2). The spatial patterns  
5 308 of changes are consistent across different scenarios and time periods, but the size of  
6 309 changes varies (Figure S5). The uncertainty across crop yield projections (standard  
7 310 deviation of CVs across all 8 emulators and 21 GCMs) ranged between 17%-119% with  
8 311 the CO<sub>2</sub> fertilization effect, with a global mean of 39% under RCP8.5-2080s.  
9 312 Uncertainty was most pronounced in central Europe to eastern Russia, and in the  
10 313 northern Indian production regions (Figure S6). We further break the total uncertainty  
11 314 to those associated with the emulators and those with the GCMs, by analysis of variance.  
12 315 Disagreement across the emulators explained less than 50% of the total variance in 47%  
13 316 of the harvested areas (Figure S7).





318

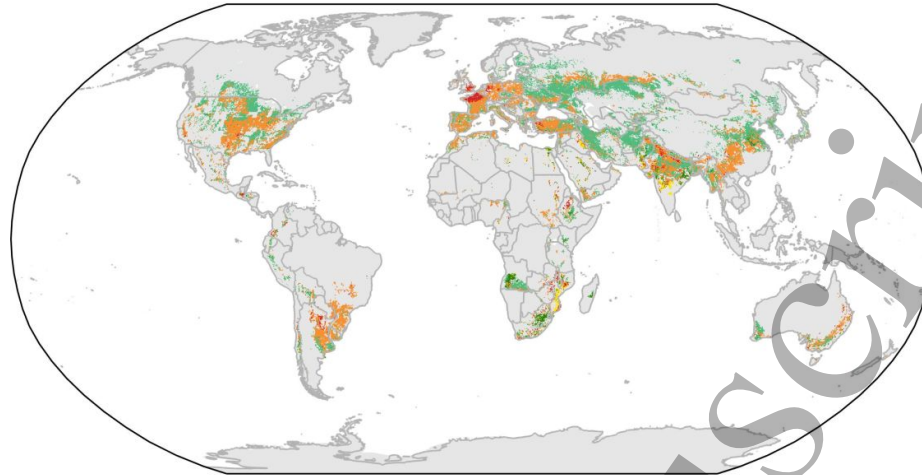
319 **Figure 2** Changes in wheat yield CV (RCP4.5-2080s and RCP8.5-2080s) relative to the baseline (1976-  
 320 2005) based on the median of 21 GCMs and 8 crop model emulators using perturbations of temperature,  
 321 precipitation, and CO<sub>2</sub> concentration according to RCP4.5 and RCP8.5 ("T+P+CO<sub>2</sub>").

322

323 Changes in yield CV are linked to changes in mean yield and yield standard deviation.

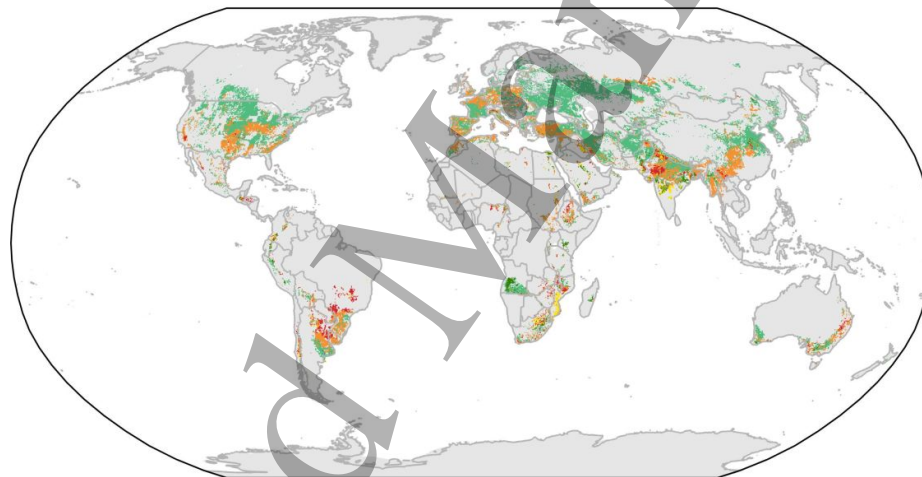
324 Under RCP8.5-2080s, mean yield levels increase in 92.1% of harvested areas and the  
 325 yield standard deviation increases in 95.3% of harvested areas (Figure S8). 30.8% of  
 326 the areas in which CV is found to increase, CV changes are dominated by increases in  
 327 yield standard deviation ( $|SD+| > |MY+|$ ). In regions where CV is decreasing, 59.3% of  
 328 the areas are dominated by mean yield increases ( $|SD+| < |MY+|$ ) (Figure 3, Table 2).

329 Under RCP4.5-2080s, mean yield levels and the yield standard deviation increase in  
 330 92.8% and 94.5% of the harvested areas, respectively (Figure S8). 42.7% of the areas  
 331 in which CV is found to increase, CV changes are dominated by increases in yield  
 332 standard deviation ( $|SD+| > |MY+|$ ). In regions where CV is decreasing, 47.6% of the  
 333 areas are dominated by mean yield increases ( $|SD+| < |MY+|$ ) (Figure 3, Table 2).



SD+ & MY- |SD+| > |MY+| |SD-| < |MY-| |SD+| < |MY+| |SD-| > |MY-| SD- & MY+  
 CV+ under RCP4.5-2080s CV- under RCP4.5-2080s

334



SD+ & MY- |SD+| > |MY+| |SD-| < |MY-| |SD+| < |MY+| |SD-| > |MY-| SD- & MY+  
 CV+ under RCP8.5-2080s CV- under RCP8.5-2080s

335

336 **Figure 3** Factors of yield CV changes, including mean yield changes (MY) and yield standard  
 337 deviation changes (SD). Positive changes are indicated with “+” and negative changes with “-”. The  
 338 |MY+| and |SD+| denote the absolute increase of mean yield and yield standard deviation, respectively.

339

340 **Table 2** Attribution of wheat harvested area with yield CV changes to changes in mean yield (MY) and  
 341 standard deviation (SD) under RCP4.5-2080s and RCP8.5-2080s.

Changes in yield CV	Category of SD and MY change	Fraction of harvested areas	
		RCP4.5	RCP8.5
CV+	SD+ & MY-	4.3%	5.2%
	SD+  >  MY+	42.7%	30.8%
	SD-  <  MY-	2%	0.6%



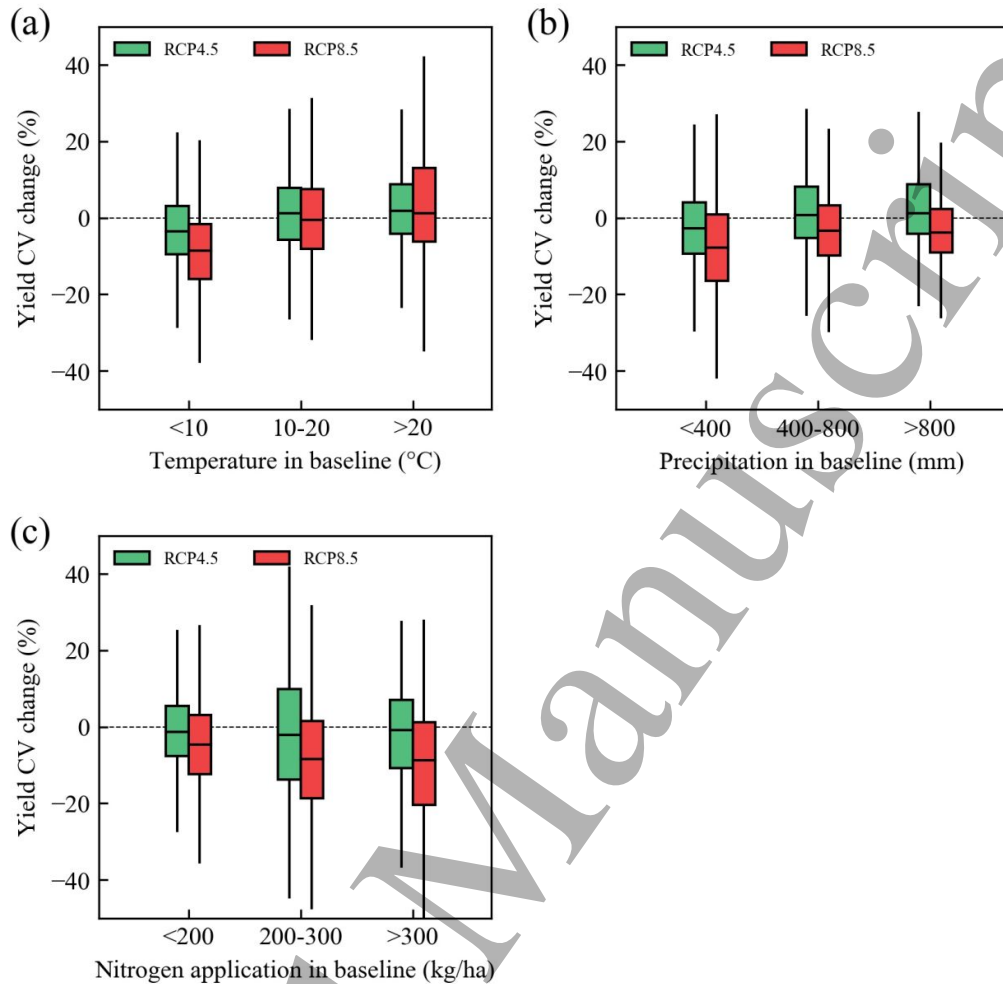
	SD+  <  MY+	47.6%	59.3%
CV-	SD-  >  MY-	0.9%	2.1%
	SD- & MY+	2.6%	2.0%

342 \* “+” denotes positive changes, and the “-” denotes negative changes. “|SD+| > |MY+|” denotes the  
 343 absolute value of increase in yield SD is greater than that in the mean yield.  
 344

### 345 3.2 Changes in the yield CV across different climatic regions

346 Changes in the wheat yield CV exhibited a clear relationship with the baseline regional  
 347 temperature, precipitation, and nitrogen fertilizer application rate. In general, regions  
 348 with hotter growing seasons (growing season average temperature >20 °C) or with  
 349 lower nitrogen fertilizer application rates (nitrogen application rate < 200kg/ha),  
 350 experienced the largest relative increase in wheat yield CV (Figure 4).

351  
 352 The increases in yield CV tend to be greater in regions with hotter growing seasons  
 353 under both RCP4.5 and RCP8.5, including sub-Saharan Africa, India, Australia’s wheat  
 354 belt, South East US, and southern Brazil and Argentina. These are regions in which  
 355 mean wheat yields are expected to decrease under high-emission climate change  
 356 scenarios, whereas at higher latitudes with lower growing season temperatures mean  
 357 wheat yields are generally projected to increase (Jägermeyr *et al* 2021). The change in  
 358 yield CV undergoes smaller decline under RCP8.5 and even experiences subtle increase  
 359 under RCP4.5 in regions with wetter growing seasons, which can be attributed to  
 360 stronger variability of precipitation in wetter regions. Underperforming wheat  
 361 production system regions, like Brazil, sub-Saharan Africa, and South East Asia, with  
 362 lower levels of nitrogen application, are likely to experience a greater increase in yield  
 363 CV under both RCP4.5 and RCP8.5.



364

365

366

367

368

369

370

371

372

373

374

375

376

377

378

379

380

381

382

383

384

385

386

387

388

389

390

391

392

**Figure 4** Wheat yield CV change under RCP4.5 and RCP8.5, separated by different climatic and management bins: growing season mean temperature (a), growing season total precipitation (b), and nitrogen fertilizer application (c). The bin classification refers to baseline reference conditions. CV change is based on the T+P+CO<sub>2</sub> simulations. Box-and-whisker plots show the distribution of yield CV changes across all cultivated grid cells in each class. The group divisions are based on approximately equal sample sizes.

### 3.3 Climatic drivers of and their relative contributions to the change in yield CV

In simulations based on individual climate drivers, temperature changes alone increase the yield CV for 55% and 56% of the harvested areas under RCP4.5-2080s and RCP8.5-2080s, respectively. Under RCP8.5-2080s the magnitude of increased yield CV with temperature change alone is larger than that with precipitation change alone, but the extent of the area affected by increasing yield CV is smaller (Figure 5). The yield CV increases in 64% and 60% of harvested areas when only precipitation change is

379 assumed under RCP4.5-2080s and RCP8.5-2080s, respectively (Figure 5).

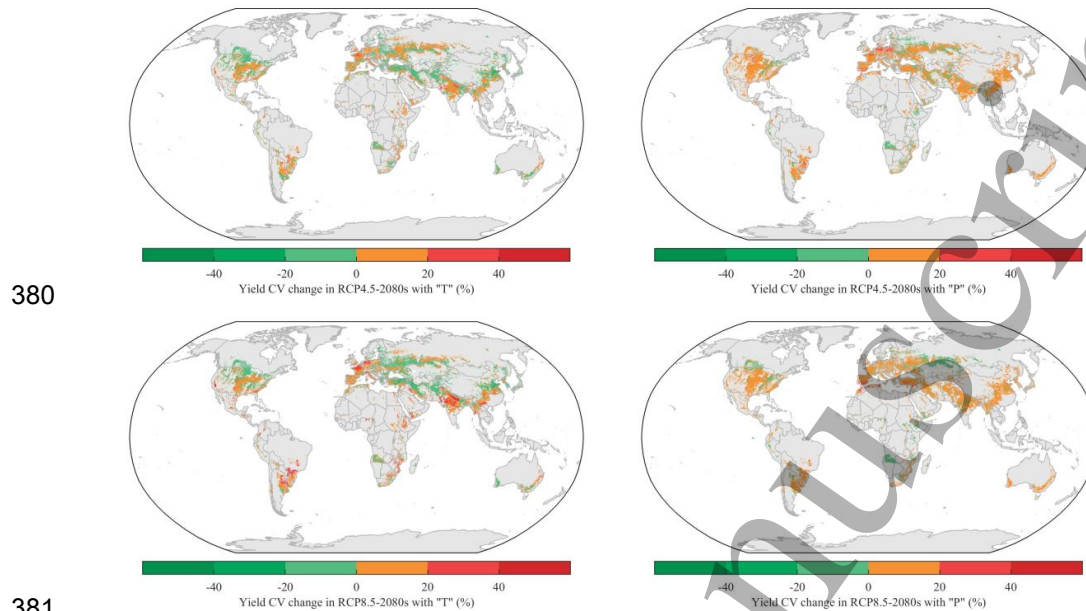
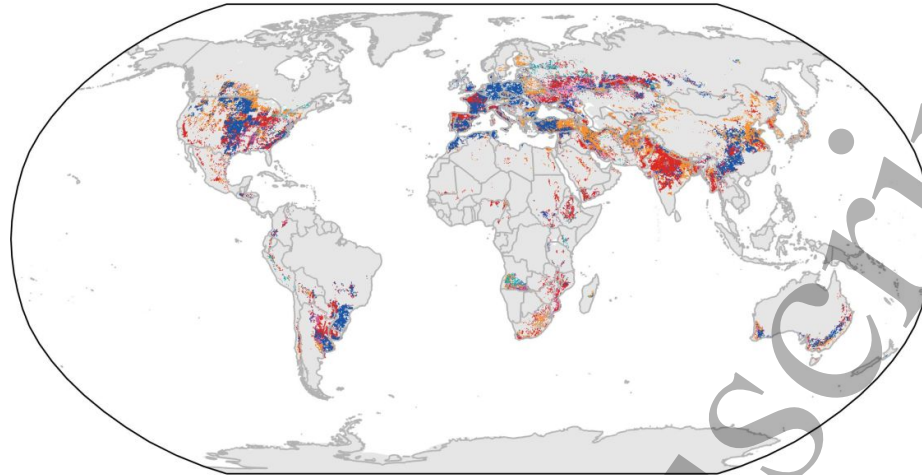


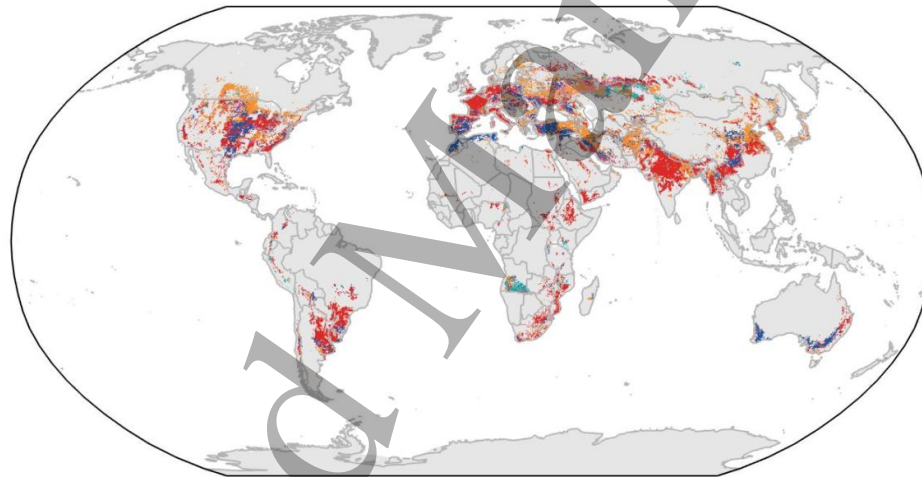
**Figure 5** Changes in yield CV under isolated temperature and precipitation perturbations (RCP4.5-2080s and RCP8.5-2080s). Yield CV changes are shown as the median of 21 GCMs and 8 crop model emulators. “T” is the effect of temperature change, and “P” is the effect of precipitation change.

After separating the relative contributions of climate drivers under RCP4.5-2080s, precipitation was the dominant driver to increase the yield CV in 33% of harvested areas, even if the temperature change plays a more important role in yield CV change in over half of harvested areas (53%). The interaction between temperature and precipitation change played a dominant role in changes in yield CV in 10% of harvested areas. Under RCP8.5-2080s, temperature becomes a more important factor and was found to be the dominant driver in 72% of global wheat harvested areas, of which, yield CV increased in 41% of harvested areas. Precipitation was found to be the dominant driver in 21% of harvested areas, of which, yield CV increased in 17% of harvested areas. The interaction between temperature and precipitation played a dominant role in the change in yield CV in only 8% harvested areas (Figure 6).



Temperature+ Temperature- Precipitation+ Precipitation- Interaction+ Interaction-  
 Spatial distribution of dominant factors in RCP4.5-2080s

397



Temperature+ Temperature- Precipitation+ Precipitation- Interaction+ Interaction-  
 Spatial distribution of dominant factors in RCP8.5-2080s

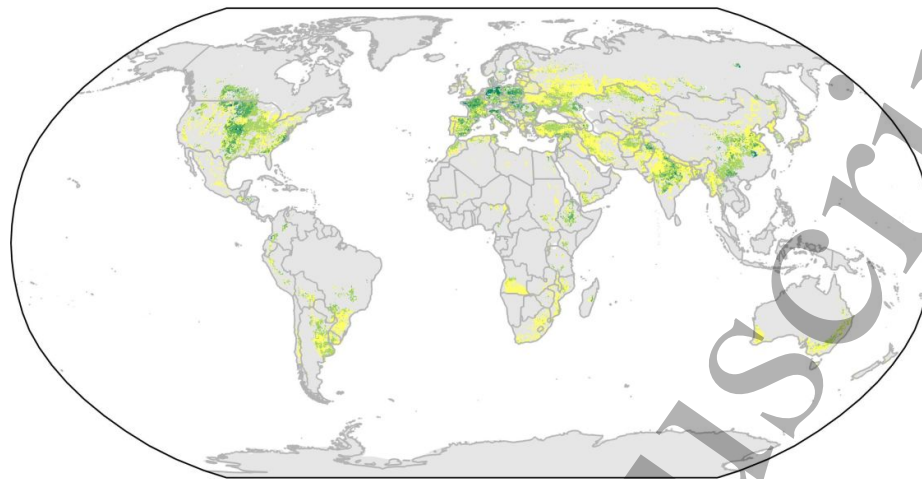
398

399 **Figure 6** Major contributors to the change in wheat yield CV (RCP4.5-2080s and RCP8.5-2080s). The  
 400 dominant factors driving the change in yield CV are defined as the driving factors that contribute the  
 401 most to the increase (or decrease) in the yield CV in each grid cell. The suffix '+' attached to the driving  
 402 factor name indicates increase in the CV, whereas a '-' indicates a reduction in the CV.

403

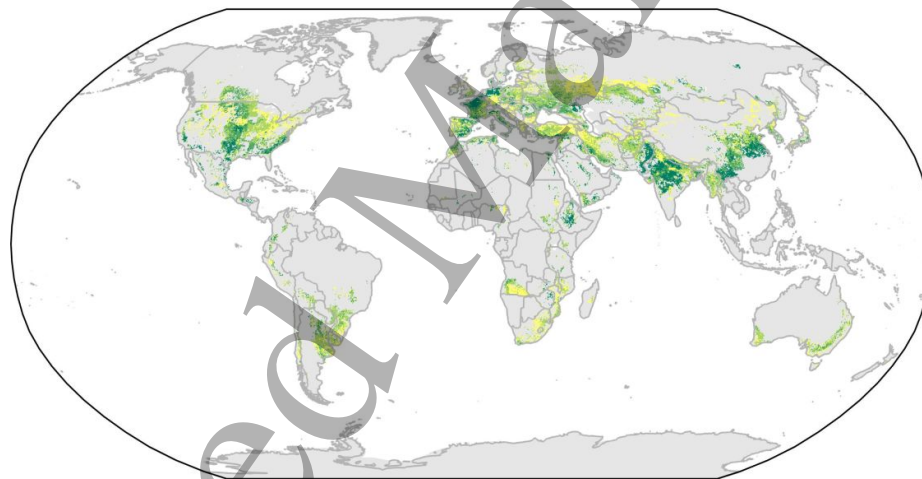
404 The elevated CO<sub>2</sub> concentration reduced the increase in yield CV, which was greatest  
 405 in RCP8.5-2080s. The effect was strongest (>15%) in central Europe, south Asia, North  
 406 and Southwest China, and North America. The mitigation effect was weaker under the  
 407 other RCP4.5-2080s, but the spatial patterns were largely consistent with RCP8.5-

1  
2  
3  
4 408 2080s (Figure 7).  
5  
6  
7  
8  
9  
10  
11  
12  
13  
14  
15  
16  
17  
18  
19



20  
21  
22 Reduction of yield CV by CO<sub>2</sub> fertilization in RCP4.5-2080s (%)  
23

24 409



25  
26  
27  
28  
29  
30  
31  
32  
33  
34  
35  
36  
37  
38  
39  
40  
41  
42 Reduction of yield CV by CO<sub>2</sub> fertilization in RCP8.5-2080s (%)  
43

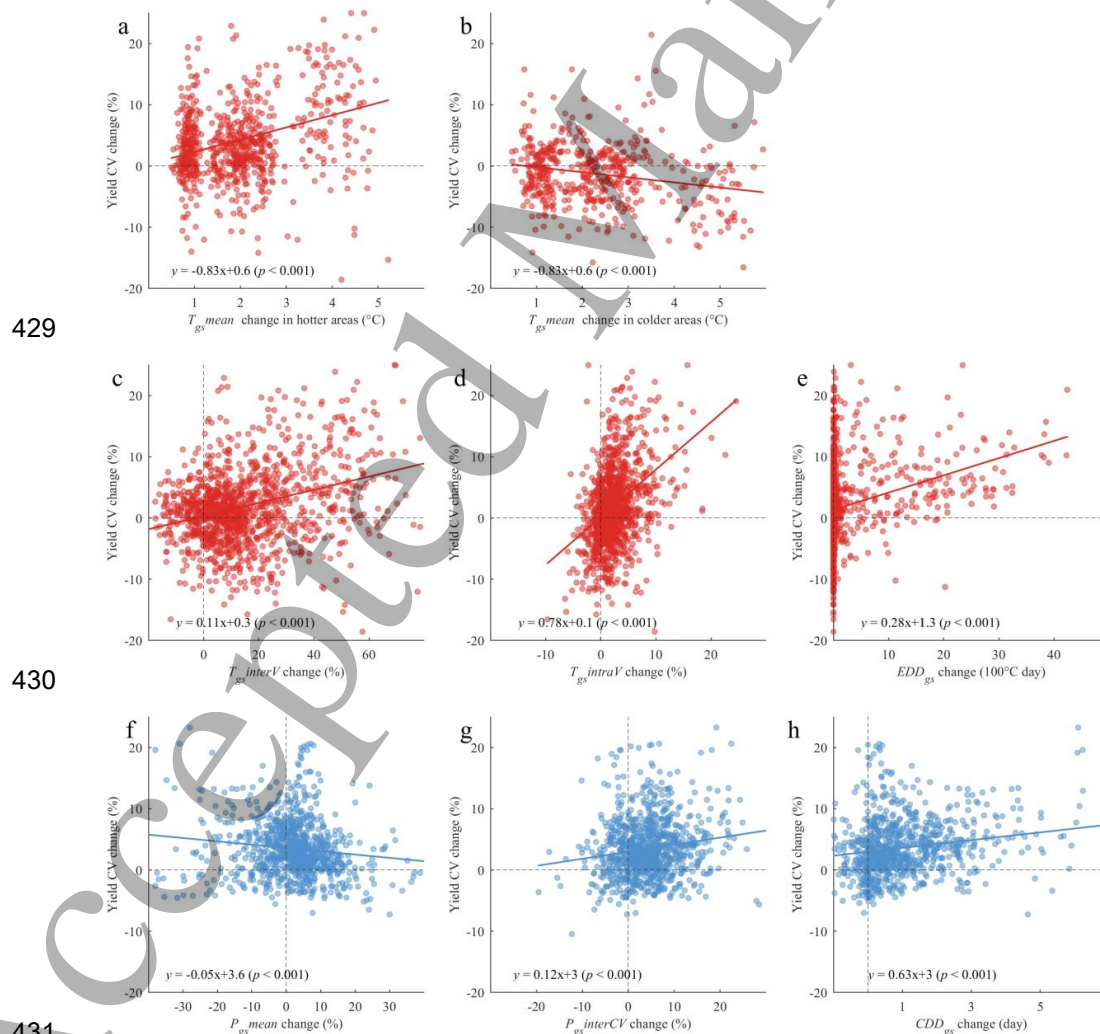
44

45  
46  
47  
48  
49  
50  
51  
52  
53  
54  
55  
56  
57  
58  
59  
60

410  
411 **Figure 7** Reduction effect (“T+P+CO<sub>2</sub>” - “T+P”) on change in yield CV from CO<sub>2</sub> fertilization.  
412

413 To elucidate the link between changes in yield CV and climate factors, we further  
414 examined the change in yield CV with climatic factors changes in mean, variability,  
415 and extremes of temperature and precipitation by using perturbation “T” and “P” results.  
416 A linear regression was conducted between median changes in yield CV and growing  
417 season climatic factors from food producing units (FPUs, Kummu *et al.*, 2010) (Figure

418 8). The change in yield CV was positively correlated with change in interannual  
 419 variability ( $T_{gs}interV$ , Figure 8-c), intra-seasonal variability ( $T_{gs}intraV$ , Figure 8-d), and  
 420 extreme degree day ( $EDD_{gs}$ , Figure 8-e) of temperature. The relationship between mean  
 421 temperature and yield CV varied by region. For regions with hotter growing seasons  
 422 ( $T_{gs}mean > 10^{\circ}C$ , Figure 8-a), a warming trend tended to increase the yield CV, and  
 423 decrease the yield CV in regions with colder growing season ( $T_{gs}mean < 10^{\circ}C$ , Figure  
 424 8-b). For the effect of precipitation change, results from grid cells with rainfed systems  
 425 showed that change in yield CV was negatively correlated with change in total  
 426 precipitation ( $P_{gs}mean$ , Figure 8-f), but positively correlated with interannual  
 427 variability of precipitation ( $P_{gs}interCV$ , Figure 8-g), and drought intensity (consecutive  
 428 drought days,  $CDD_{gs}$ , Figure 8-h), all statistically significant.



1  
2  
3 **Figure 8** Correlations of changes in yield CV with the changes in mean, variability, and extremes of  
4 temperature and precipitation at the FPU level relative to the baseline. In each panel, the changes in  
5 growing season climate factor are: (a) mean temperature (baseline value > 10°C), (b) mean temperature  
6 (baseline value < 10°C), (c) interannual variability (standard deviation) of mean temperature, (d) intra-  
7 season variation of daily temperature, (e) extreme degree days, (f) total precipitation, (g) interannual  
8 variability (coefficient of variation) of precipitation, and (h) consecutive drought days.  
9

## 10 11 12 **4. Discussion**

### 13 14 15 16 **4.1 Changes in future wheat yield variability**

17  
18  
19 Our results indicate that wheat yield CV might increase significantly in 18% of the  
20 global harvested area under a high-emission climate change scenario. In turn, yield  
21 variability is found to decrease in 44% of currently cultivated areas, regions in which  
22 variability is found to decrease in 44% of currently cultivated areas, regions in which  
23 mean yields are projected to increase under climate change. Globally, our findings are  
24 consistent with those of earlier studies indicating that declining yield variability is wide-  
25 spread but increasing yield variability is found across important breadbasket regions  
26 (Iizumi and Ramankutty 2016, Leng 2017). Site-based simulation results for a 2°C  
27 warming scenario (Liu *et al.*, 2019) have provided a more pessimistic estimation, with  
28 wheat yield CV increases in 36 out of the 60 sites, including the CO<sub>2</sub> fertilization effect.  
29 Our results confirm higher yield variability in hot regions as reported by (Liu *et al.*,  
30 2019) and in regions with low nitrogen fertilizer application rates as reported by (Han  
31 *et al.*, 2020). Similarly, the low yield CV in high nitrogen fertilizer application rates  
32 regions is consistent with the findings of nutrients-driven intensification that additional  
33 nutrient inputs raise mean crop yields and thus decrease yield CV (Müller *et al* 2018).  
34  
35

36  
37  
38 A detailed comparison of yield CV changes between site-based projections (Liu *et al*  
39 2019b) and our gridded projections demonstrates the importance of revealing spatial  
40 heterogeneity of yield variability changes. Changes in yield CV were identified as  
41 significantly increasing at all 14 sites for the 2°C warming scenario (Liu *et al.*, 2019).  
42  
43  
44 Among the 14 sites, our estimates were consistent with 10 of the 14 stations. For the  
45  
46  
47  
48  
49  
50  
51  
52  
53  
54  
55  
56  
57  
58  
59  
60

1  
2  
3 460 other 46 sites, our results are largely consistent with the 25 sites across the central U.S.,  
4  
5 461 South America, the Middle East, the western European coastline, and Southern Russia;  
6  
7 462 but are different in the direction of change for other sites. Spatial heterogeneous yield  
8  
9 463 variability changes are the main cause of inconsistency between our projections and Liu  
10  
11 464 *et al.* (2019). This is the case in Glen and Bloemfontein in South Africa, and Dharwar  
12  
13 465 in India for the four inconsistent sites, as well as 11 out of the other 21 inconsistent  
14  
15 466 sites, including those in northwest US, around the western or northern coast of the Black  
16  
17 467 Sea, in central southern Russia, North China, and south-eastern Australia. Besides,  
18  
19 468 another cause may be the choice of the crop model ensemble and underlying  
20  
21 469 uncertainties. We examined our results for each crop model emulator. The direction of  
22  
23 470 each site-based change in yield CV reported by Liu *et al.* (2019) can be found in the  
24  
25 471 result of at least one of our emulators, indicating GCMs-crop models ensemble  
26  
27 472 combination is critical to yield projection.

28 473

29 474 Spatial heterogeneity of crop yield variability creates a huge challenge for agricultural  
30  
31 475 risk management (Benami *et al* 2021). The spatially heterogeneous yield CV changes  
32  
33 476 are also found in earlier reports that yield variability changes in rice and wheat are  
34  
35 477 sensitive to spatial resolution (Iizumi *et al* 2018). Previous yield variability projections  
36  
37 478 conducted with site-based, process-based models have found that regional yield  
38  
39 479 variability changes are not consistent across different sites (Liu *et al* 2020). Thus, the  
40  
41 480 gridded process-based crop models can provide an overview of global or regional  
42  
43 481 changes in yield variability (Parkes *et al* 2018, Ostberg *et al* 2018). The ability to  
44  
45 482 represent this spatial heterogeneity in yield variability in light-weight emulators allows  
46  
47 483 for more comprehensive assessments of the risk of changes in yield variability.

#### 48 484 **4.2 Climatic drivers of changes in future wheat yield variability**

50  
51 485 The present results indicate strong links between changes in the wheat yield CV  
52  
53 486 and changes in temperature and precipitation. Previous reports have suggested that  
54  
55 487 changes in yield interannual variability are closely related to changes in the variability



1  
2  
3 488 (both interannual and intra-seasonal) (Iizumi *et al.*, 2013; Peng *et al.*, 2018) and  
4 489 extremes of climate factors (Chen *et al.*, 2018; Iizumi and Ramankutty, 2016). In  
5  
6 490 addition, due to the non-linear relationship between yield and temperature, changes in  
7  
8 491 the mean temperature, away from the optimal range, will increase the interannual yield  
9  
10 492 CV (Urban *et al.*, 2012; Tigchelaar *et al.*, 2018). The response of the interannual yield  
11  
12 493 variability to changes in precipitation is more complex than for temperature. In general,  
13  
14 494 changes in precipitation have smaller effects on irrigated yield than on rainfed yield  
15  
16 495 (Kothari *et al.*, 2019; Tubiello *et al.*, 2002). In rainfed systems, yield interannual  
17  
18 496 variability has been known to be closely related to interannual variability of rainfall, as  
19  
20 497 well as frequency and intensity of drought (Webber *et al.*, 2018). The effect of total  
21  
22 498 precipitation change largely depends on the baseline humidity of the production region.  
23  
24 499 For drylands, increasing total precipitation increases mean yield (Fronzek *et al.*, 2018)  
25  
26 500 and consequently reduces CV. Also, the interaction between temperature and  
27  
28 501 precipitation changes can mitigate the increase in yield CV, although the magnitude of  
29  
30 502 the interaction effect on change in yield CV is modest, within 10%. This is similar to  
31  
32 503 the mitigation effect of irrigation on heat stress (Zaveri and B. Lobell, 2019). However,  
33  
34 504 the interaction effect cannot be explicitly explained, depending on the timing, intensity,  
35  
36 505 and volume of rainfall (Tack *et al.*, 2017).

37  
38 506  
39  
40 507 Higher atmospheric CO<sub>2</sub> concentrations mitigate variability changes in crop yield  
41  
42 508 (Urban *et al.*, 2015), a consistent finding across different scenarios and time periods  
43  
44 509 (Figure 7). The mitigation effect is mainly attributed to increases in mean crop yield  
45  
46 510 under elevated CO<sub>2</sub>. Wheat as a C3 crop is known to have a high capacity to benefit  
47  
48 511 from elevated CO<sub>2</sub> levels, which has been confirmed by various previous experiment-  
49  
50 512 based evidences (Kimball 2016, Toreti *et al* 2020) . Negative effects of global warming  
51  
52 513 on future wheat yield could potentially be fully compensated by yield-amplifying  
53  
54 514 effects of elevated atmospheric CO<sub>2</sub> concentrations (Ye *et al.*, 2020).

### 515 4.3 Uncertainties

516 The spatial pattern of uncertainty in our results is consistent with different uncertainty  
517 distribution between high and low latitudes provided by crop model simulation (Xiong  
518 *et al* 2020). Including the CO<sub>2</sub> fertilization effect would further increase the total size  
519 of uncertainty in the projected yield. This is in agreement with a recent analysis on  
520 sources of uncertainty regarding GCMs and GGCM statistical emulators (Müller *et al.*,  
521 2021).

522  
523 The use of emulator ensemble simulation enabled the estimation of wheat yield  
524 variability change driven by climate change. Nevertheless, our approach has two  
525 limitations. First, crop damage from climate extremes is a major driving force of  
526 interannual yield variability (Trnka *et al.*, 2014), but the capability of most crop models  
527 in reproducing extreme climate damage to crops is still limited (Rötter *et al.*, 2018). For  
528 instance, process-based crop models of the GGCM phase 1 experiment fail to  
529 reproduce yield impact from too wet conditions (Li *et al* 2019). Also, process-based  
530 crop models underestimate the extremeness of the 2003 heat-drought (Schewe *et al*  
531 2019). We employ newly developed crop model emulators to project future wheat yield  
532 and these emulators are capable of capturing the direction of yield anomalies due to  
533 climate extremes, indicating the type of extreme event-induced yield variability that is  
534 captured by the models (heat, drought) will increase yield variability in a fair share of  
535 current cropland. Second, interannual yield variability driven by non-climatic factors is  
536 not considered in our analysis. These non-climatic factors can strongly affect yield  
537 variability (Albers *et al* 2017) and changes in management can also strongly affect yield  
538 levels under climate change (Minoli *et al* 2019, Zabel *et al* 2021).

### 539 4.4 Implications

540 The spatial scale of our estimates reached the sub-province scale in China and the sub-  
541 state scale in the US and thus provided more insight than previous global estimates.

1  
2  
3 542 First, gridded estimated yield variability change could provide more detail on spatial  
4 543 heterogeneity in local areas. Such local spatial differences were pronounced in South  
5 544 Africa, eastern Africa, and Central Russia. Second, when there is a need to estimate  
6 545 regional or country-level aggregated yield variability change, our gridded estimates  
7 546 could enable straightforward aggregation rather than upscaling from site-based  
8 547 estimates—these estimates rely heavily on the representativeness of sites.  
9  
10  
11  
12  
13

14 548

15  
16 549 High-spatial resolution gridded estimates of future yield variability change enabled  
17 550 global estimates of future change in yield CV. Globally, changes in yield CV tend to  
18 551 decrease in 44% of global harvested areas; but still yields would become more unstable  
19 552 in 18% of global harvested areas under RCP8.5-2080s, including several major  
20 553 production regions and countries. This indicates potential challenges to the stability of  
21 554 grain supply, market pricing, and consequently, the whole food system in the context  
22 555 of future climate change. It is important for local and regional economies to proactively  
23 556 implement adaptation measures and policy support (Iizumi and Ramankutty, 2016). In  
24 557 light of this, our results can provide details of spatial heterogeneity in local areas and  
25 558 identify regions with urgent needs, including those hot and low-fertilizer application  
26 559 regions. The predominant climate driver is also identified, so that adaptation strategies  
27 560 can be tailored for regional or local challenges.  
28  
29  
30  
31  
32  
33  
34  
35  
36  
37

38 561

39  
40 562 To face the challenge of increased yield interannual variability, adaptations including  
41 563 mean-increasing and variance-reducing strategies (Mehrabi and Ramankutty, 2019),  
42 564 are needed because the changes in relative yield variability (CV) are sourced from both  
43 565 changes in mean yield and yield standard deviation (Figure S9). The focus on the  
44 566 relative yield variability (CV) rather than absolute (e.g. SD) reflects the producer  
45 567 perspective, where the variability around the mean is relevant (storage, financial buffers)  
46 568 even if the mean is increasing in the long-term. Shifting cultivars (Olmstead and Rhode,  
47 569 2011; Liu *et al.*, 2010) and adjusting planting dates (Lobell, 2014; Huang *et al.*, 2020)  
48  
49  
50  
51  
52  
53  
54 570 have been recognized as effective adaptation options to address heat stress. Likewise,  
55  
56  
57  
58  
59  
60

1  
2  
3 571 reinforcing irrigation equipment and adjusting irrigation strategies could relieve water  
4  
5 572 shortages (Zhao *et al.*, 2020). Additionally, increasing nitrogen application rates in  
6  
7 573 underperforming wheat production system regions could mitigate the increase in yield  
8  
9 574 CV (Han *et al.*, 2020). From a risk management perspective, the risk in increased yield  
10  
11 575 CV requires better domestic inter-temporal reserves of wheat grain to smooth  
12  
13 576 fluctuations in interannual production, market supply, and commodity price and better  
14  
15 577 financial buffers at the producer level, to mitigate financial losses from local less-than-  
16  
17 578 average yields.

## 19 20 579 **5. Conclusions**

21  
22  
23 580 This study presents one of the first projections of future wheat yield interannual  
24  
25 581 variability change at high spatial resolution and disentangles the impacts from changes  
26  
27 582 in temperature, precipitation, and CO<sub>2</sub> on those changes. Our results reveal that future  
28  
29 583 climate change alters wheat yield interannual variability in over 60% of harvested areas.  
30  
31 584 Wheat yield variability may decrease in over 40% of global wheat harvested areas under  
32  
33 585 a high-emission climate change scenario (RCP8.5-2080s), while under RCP4.5-2080s  
34  
35 586 only 31% of harvested areas undergo the declined yield CV. However, 23% and 18%  
36  
37 587 of harvested areas experience increased yield CV under RCP4.5-2080s and RCP8.5-  
38  
39 588 2080s, respectively. Greater increase in yield standard deviation than that in the mean  
40  
41 589 yield was the main reason for the increase yield variability under both RCP4.5 and  
42  
43 590 RCP8.5. Yields in hotter or lower fertilizer regions are projected to become more  
44  
45 591 unstable. Worldwide, changes in temperature have a stronger influence on changes in  
46  
47 592 yield variability compared with precipitation in 72% of global harvested areas under  
48  
49 593 RCP8.5-2080s, whereas under RCP4.5-2080s the areas controlled by temperature  
50  
51 594 changes are smaller (predominant in 53% of harvested areas). The global mean of yield  
52  
53 595 CV reduction due to rising CO<sub>2</sub> concentration across current harvested areas are 5%  
54  
55 596 and 8% under RCP4.5-2080s and RCP8.5-2080s, respectively. High spatial resolution  
56  
57 597 patterns of changes in wheat yield variability, as well as site-specific major driver

1  
2  
3 598 identification results, have great implications for policy-making with regard to where  
4  
5 599 food supply and farmer income need to be stabilized by additional measures in wheat  
6  
7 600 production throughout the world.  
8  
9 601

10 602 **Acknowledgment:** This study was supported by National Key R&D Program of China  
11  
12 603 (No. 2016YFA0602404)  
13  
14 604

15  
16  
17  
18  
19  
20  
21  
22  
23  
24  
25  
26  
27  
28  
29  
30  
31  
32  
33  
34  
35  
36  
37  
38  
39  
40  
41  
42  
43  
44  
45  
46  
47  
48  
49  
50  
51  
52  
53  
54  
55  
56  
57  
58  
59  
60

605 **References**

- 606 Albers H, Gornott C and Hüttl S 2017 How do inputs and weather drive wheat yield volatility? The  
607 example of Germany *Food Policy* **70** 50–61 Online:  
608 <http://dx.doi.org/10.1016/j.foodpol.2017.05.001>
- 609 Ben-Ari T, Boé J, Ciais P, Lecerf R, Van Der Velde M and Makowski D 2018 Causes and implications  
610 of the unforeseen 2016 extreme yield loss in the breadbasket of France *Nat. Commun.* **9** 1627  
611 Online: <http://dx.doi.org/10.1038/s41467-018-04087-x>
- 612 Benami E, Jin Z, Carter M R, Ghosh A, Hijmans R J, Hobbs A, Kenduywo B and Lobell D B 2021  
613 Uniting remote sensing, crop modelling and economics for agricultural risk management *Nat.*  
614 *Rev. Earth Environ.* **2** 140–59 Online: <http://dx.doi.org/10.1038/s43017-020-00122-y>
- 615 Blanc É 2017 Statistical emulators of maize, rice, soybean and wheat yields from global gridded crop  
616 models *Agric. For. Meteorol.* **236** 145–61
- 617 Blanc E and Sultan B 2015 Emulating maize yields from global gridded crop models using statistical  
618 estimates *Agric. For. Meteorol.* **214–215** 134–47
- 619 Ceglar A, Toreti A, Lecerf R, Van der Velde M and Dentener F 2016 Impact of meteorological drivers  
620 on regional inter-annual crop yield variability in France *Agric. For. Meteorol.* **216** 58–67
- 621 Challinor A J, Watson J, Lobell D B, Howden S M, Smith D R and Chhetri N 2014 A meta-analysis of  
622 crop yield under climate change and adaptation *Nat. Clim. Chang.* **4** 287–91
- 623 Chen Y, Zhang Z and Tao F 2018 Impacts of climate change and climate extremes on major crops  
624 productivity in China at a global warming of 1.5 and 2.0°C *Earth Syst. Dyn.* **9** 543–62
- 625 Döring T F and Reckling M 2018 Detecting global trends of cereal yield stability by adjusting the  
626 coefficient of variation *Eur. J. Agron.* **99** 30–6 Online: <https://doi.org/10.1016/j.eja.2018.06.007>
- 627 Elliott J, Müller C, Deryng D, Chryssanthacopoulos J, Boote K J, Büchner M, Foster I, Glotter M,  
628 Heinke J, Iizumi T, Izaurralde R C, Mueller N D, Ray D K, Rosenzweig C, Ruane A C and  
629 Sheffield J 2015 The Global Gridded Crop Model Intercomparison: data and modeling protocols  
630 for Phase 1 (v1.0) *Geosci. Model Dev.* **8** 261–77 Online: [https://www.geosci-model-](https://www.geosci-model-dev.net/8/261/2015/)  
631 [dev.net/8/261/2015/](https://www.geosci-model-dev.net/8/261/2015/)
- 632 FAO 2019 *World Food and Agriculture Statistical Pocketbook*
- 633 Folberth C, Baklanov A, Balković J, Skalský R, Khabarov N and Obersteiner M 2019 Spatio-temporal  
634 downscaling of gridded crop model yield estimates based on machine learning *Agric. For.*  
635 *Meteorol.* **264** 1–15
- 636 Franke J A, Müller C, Elliott J, Ruane A C, Jägermeyr J, Balkovic J, Ciais P, Dury M, Falloon P D,  
637 Folberth C, François L, Hank T, Hoffmann M, Izaurralde R C, Jacquemin I, Jones C, Khabarov  
638 N, Koch M, Li M, Liu W, Olin S, Phillips M, Pugh T A M, Reddy A, Wang X, Williams K,  
639 Zabel F and Moyer E J 2020a The GGCM Phase 2 emulator: Global gridded crop model  
640 simulations under uniform changes in CO<sub>2</sub>, temperature, water, and nitrogen levels (protocol  
641 version 1.0) *Geosci. Model Dev.* **13** 2315–36
- 642 Franke J A, Müller C, Elliott J, Ruane A C, Jägermeyr J, Balkovic J, Ciais P, Dury M, Falloon P D,  
643 Folberth C, François L, Hank T, Hoffmann M, Izaurralde R C, Jacquemin I, Jones C, Khabarov  
644 N, Koch M, Li M, Liu W, Olin S, Phillips M, Pugh T A M, Reddy A, Wang X, Williams K,  
645 Zabel F and Moyer E J 2020b The GGCM Phase 2 experiment: Global gridded crop model

- 1  
2  
3 646 simulations under uniform changes in CO<sub>2</sub>, temperature, water, and nitrogen levels (protocol  
4 647 version 1.0) *Geosci. Model Dev.* **13** 2315–36
- 5 648 Fronzek S, Pirttioja N, Carter T R, Bindi M, Hoffmann H, Palosuo T, Ruiz-Ramos M, Tao F, Trnka M,  
6 649 Acutis M, Asseng S, Baranowski P, Basso B, Bodin P, Buis S, Cammarano D, Deligios P,  
7 650 Destain M F, Dumont B, Ewert F, Ferrise R, François L, Gaiser T, Hlavinka P, Jacquemin I,  
8 651 Kersebaum K C, Kollas C, Krzyszczak J, Lorite I J, Minet J, Minguez M I, Montesino M,  
9 652 Moriondo M, Müller C, Nendel C, Öztürk I, Perego A, Rodríguez A, Ruane A C, Ruget F, Sanna  
10 653 M, Semenov M A, Slawinski C, Stratonovitch P, Supit I, Waha K, Wang E, Wu L, Zhao Z and  
11 654 Rötter R P 2018 Classifying multi-model wheat yield impact response surfaces showing  
12 655 sensitivity to temperature and precipitation change *Agric. Syst.* **159** 209–24
- 13 656 Han X, Hu C, Chen Y, Qiao Y, Liu D, Fan J, Li S and Zhang Z 2020 Crop yield stability and  
14 657 sustainability in a rice-wheat cropping system based on 34-year field experiment *Eur. J. Agron.*  
15 658 **113** 125965 Online: <https://doi.org/10.1016/j.eja.2019.125965>
- 16 659 Hawkins E, Fricker T E, Challinor A J, Ferro C A T, Ho C K and Osborne T M 2013 Increasing  
17 660 influence of heat stress on French maize yields from the 1960s to the 2030s *Glob. Chang. Biol.*  
18 661 **19** 937–47
- 19 662 Holzkämper A, Calanca P and Fuhrer J 2012 Statistical crop models: Predicting the effects of  
20 663 temperature and precipitation changes *Clim. Res.* **51** 11–21
- 21 664 Huang M, Wang J, Wang B, Liu D L, Yu Q, He D, Wang N and Pan X 2020 Optimizing sowing  
22 665 window and cultivar choice can boost China's maize yield under 1.5 °C and 2 °C global warming  
23 666 *Environ. Res. Lett.* **15**
- 24 667 Iizumi T, Kotoku M, Kim W, West P C, Gerber J S and Brown M E 2018 Uncertainties of potentials  
25 668 and recent changes in global yields of major crops resulting from census- and satellite-based  
26 669 yield datasets at multiple resolutions *PLoS One* **13** e0203809 Online:  
27 670 <https://doi.org/10.1371/journal.pone.0203809>
- 28 671 Iizumi T and Ramankutty N 2016 Changes in yield variability of major crops for 1981–2010 explained  
29 672 by climate change *Environ. Res. Lett.* **11** 34003 Online: [http://dx.doi.org/10.1088/1748-](http://dx.doi.org/10.1088/1748-9326/11/3/034003)  
30 673 [9326/11/3/034003](http://dx.doi.org/10.1088/1748-9326/11/3/034003)
- 31 674 Iizumi T, Sakuma H, Yokozawa M, Luo J J, Challinor A J, Brown M E, Sakurai G and Yamagata T  
32 675 2013 Prediction of seasonal climate-induced variations in global food production *Nat. Clim.*  
33 676 *Chang.* **3** 904–8
- 34 677 IPCC 2014 *Climate Change 2014: Synthesis Report*
- 35 678 IPCC 2019 *Climate Change and Land: An IPCC Special Report on climate change, desertification,*  
36 679 *land degradation, sustainable land management, food security, and greenhouse gas fluxes in*  
37 680 *terrestrial ecosystems*
- 38 681 Jägermeyr J, Müller C, Ruane A, Elliott J, Balkovic J, Castillo O, Faye B, Foster I, Folberth C, Franke  
39 682 J, Fuchs K, Guarin J, Heinke J, Hoogenboom G, Iizumi T, Jain A ., Kelly D, Khabarov N, Lange  
40 683 S, Lin T, Liu W, Mialyk O, Minol S and Rosenzweig C 2021 Climate change signal in global  
41 684 agriculture emerges earlier in new generation of climate and crop models *Nat. Food (in Revis.*  
42 685 Kimball B A 2016 Crop responses to elevated CO<sub>2</sub> and interactions with H<sub>2</sub>O, N, and temperature  
43 686 *Curr. Opin. Plant Biol.* **31** 36–43 Online: <http://dx.doi.org/10.1016/j.pbi.2016.03.006>
- 44 687 Knapp S and van der Heijden M G A 2018 A global meta-analysis of yield stability in organic and  
45 688 conservation agriculture *Nat. Commun.* **9** 1–9 Online: [http://dx.doi.org/10.1038/s41467-018-](http://dx.doi.org/10.1038/s41467-018-05956-1)  
46 689 [05956-1](http://dx.doi.org/10.1038/s41467-018-05956-1)

- 1  
2  
3 690 Kothari K, Ale S, Attia A, Rajan N, Xue Q and Munster C L 2019 Potential climate change adaptation  
4 691 strategies for winter wheat production in the Texas High Plains *Agric. Water Manag.* **225** 105764  
5 692 Online: <https://doi.org/10.1016/j.agwat.2019.105764>  
6  
7 693 Kucharik C J and Ramankutty N 2005 Trends and variability in U.S. Corn yields over the twentieth  
8 694 century *Earth Interact.* **9** 1–29  
9  
10 695 Kumm M, Ward P J, de Moel H and Varis O 2010 Is physical water scarcity a new phenomenon?  
11 696 Global assessment of water shortage over the last two millennia *Environ. Res. Lett.* **5** 34006  
12 697 Online: <http://dx.doi.org/10.1088/1748-9326/5/3/034006>  
13 698 Leng G 2017 Recent changes in county-level corn yield variability in the United States from  
14 699 observations and crop models *Sci. Total Environ.* **607–608** 683–90  
15 700 Leng G and Hall J W 2020 Predicting spatial and temporal variability in crop yields: An inter-  
16 701 comparison of machine learning, regression and process-based models *Environ. Res. Lett.* **15**  
17 702 44027  
18  
19 703 Li Y, Guan K, Schnitkey G D, DeLucia E and Peng B 2019 Excessive rainfall leads to maize yield loss  
20 704 of a comparable magnitude to extreme drought in the United States *Glob. Chang. Biol.* **25** 2325–  
21 705 37  
22  
23 706 Liu B, Martre P, Ewert F, Porter J R, Challinor A J, Müller C, Ruane A C, Waha K, Thorburn P J,  
24 707 Aggarwal P K, Ahmed M, Balkovič J, Basso B, Biernath C, Bindi M, Cammarano D, De Sanctis  
25 708 G, Dumont B, Espadafor M, Eyshi Rezaei E, Ferrise R, Garcia-Vila M, Gayler S, Gao Y, Horan  
26 709 H, Hoogenboom G, Izaurralde R C, Jones C D, Kassie B T, Kersebaum K C, Klein C, Koehler A  
27 710 K, Maiorano A, Minoli S, Montesino San Martin M, Naresh Kumar S, Nendel C, O’Leary G J,  
28 711 Palosuo T, Priesack E, Ripoche D, Rötter R P, Semenov M A, Stöckle C, Streck T, Supit I, Tao  
29 712 F, Van der Velde M, Wallach D, Wang E, Webber H, Wolf J, Xiao L, Zhang Z, Zhao Z, Zhu Y  
30 713 and Asseng S 2019a Global wheat production with 1.5 and 2.0°C above pre-industrial warming  
31 714 *Glob. Chang. Biol.* **25** 1428–44  
32  
33 715 Liu B, Martre P, Ewert F, Porter J R, Challinor A J, Müller C, Ruane A C, Waha K, Thorburn P J,  
34 716 Aggarwal P K, Ahmed M, Balkovič J, Basso B, Biernath C, Bindi M, Cammarano D, De Sanctis  
35 717 G, Dumont B, Espadafor M, Eyshi Rezaei E, Ferrise R, Garcia-Vila M, Gayler S, Gao Y, Horan  
36 718 H, Hoogenboom G, Izaurralde R C, Jones C D, Kassie B T, Kersebaum K C, Klein C, Koehler A,  
37 719 Maiorano A, Minoli S, Montesino San Martin M, Naresh Kumar S, Nendel C, O’Leary G J,  
38 720 Palosuo T, Priesack E, Ripoche D, Rötter R P, Semenov M A, Stöckle C, Streck T, Supit I, Tao  
39 721 F, Van der Velde M, Wallach D, Wang E, Webber H, Wolf J, Xiao L, Zhang Z, Zhao Z, Zhu Y  
40 722 and Asseng S 2019b Global wheat production with 1.5 and 2.0°C above pre-industrial warming  
41 723 *Glob. Chang. Biol.* **25** 1428–44  
42  
43 724 Liu W, Ye T and Shi P 2020 Decreasing wheat yield stability on the North China Plain: Relative  
44 725 contributions from climate change in mean and variability *Int. J. Climatol.* 1–14  
45  
46 726 Liu Y, Wang E, Yang X and Wang J 2010 Contributions of climatic and crop varietal changes to crop  
47 727 production in the North China Plain, since 1980s *Glob. Chang. Biol.* **16** 2287–99  
48  
49 728 Lobell D B 2014 Climate change adaptation in crop production: Beware of illusions *Glob. Food Sec.* **3**  
50 729 72–6 Online: <http://www.sciencedirect.com/science/article/pii/S2211912414000145>  
51  
52 730 Lobell D B and Burke M B 2010 On the use of statistical models to predict crop yield responses to  
53 731 climate change *Agric. For. Meteorol.* **150** 1443–52 Online:  
54 732 <http://dx.doi.org/10.1016/j.agrformet.2010.07.008>  
55  
56 733 Lobell D B, Roberts M J, Schlenker W, Braun N, Little B B, Rejesus R M and Hammer G L 2014



- 1  
2  
3 734 Greater sensitivity to drought accompanies maize yield increase in the U.S. Midwest *Science*  
4 735 (80- ). **344** 516–9
- 5 736 Lobell D B, Schlenker W and Costa-Roberts J 2011 Climate Trends and Global Crop Production Since  
6 737 1980 *Science* (80- ). **333** 616–20 Online:  
7 738 <http://science.sciencemag.org/content/333/6042/616.abstract>
- 8 739 Martre P, Wallach D, Asseng S, Ewert F, Jones J W, Rötter R P, Boote K J, Ruane A C, Thorburn P J,  
9 740 Cammarano D, Hatfield J L, Rosenzweig C, Aggarwal P K, Angulo C, Basso B, Bertuzzi P,  
10 741 Biernath C, Brisson N, Challinor A J, Doltra J, Gayler S, Goldberg R, Grant R F, Heng L,  
11 742 Hooker J, Hunt L A, Ingwersen J, Izaurrealde R C, Kersebaum K C, Müller C, Kumar S N,  
12 743 Nendel C, O’leary G, Olesen J E, Osborne T M, Palosuo T, Priesack E, Ripoche D, Semenov M  
13 744 A, Shcherbak I, Steduto P, Stöckle C O, Stratonovitch P, Streck T, Supit I, Tao F, Travasso M,  
14 745 Waha K, White J W and Wolf J 2015 Multimodel ensembles of wheat growth: Many models are  
15 746 better than one *Glob. Chang. Biol.* **21** 911–25
- 16 747 Matiu M, Ankerst D P and Menzel A 2017 Interactions between temperature and drought in global and  
17 748 regional crop yield variability during 1961–2014 *PLoS One* **12** 1–23
- 18 749 Mehrabi Z and Ramankutty N 2019 Synchronized failure of global crop production *Nat. Ecol. Evol.* **3**  
19 750 780–6
- 20 751 Minoli S, Müller C, Elliott J, Ruane A C, Jägermeyr J, Zabel F, Dury M, Folberth C, François L, Hank  
21 752 T, Jacquemin I, Liu W, Olin S and Pugh T A M 2019 Global Response Patterns of Major Rainfed  
22 753 Crops to Adaptation by Maintaining Current Growing Periods and Irrigation *Earth’s Futur.* **7**  
23 754 1464–80 Online: <https://doi.org/10.1029/2018EF001130>
- 24 755 Moriondo M, Giannakopoulos C and Bindi M 2011 Climate change impact assessment: The role of  
25 756 climate extremes in crop yield simulation *Clim. Change* **104** 679–701
- 26 757 Müller C, Elliott J, Chrystanthopoulos J, Arneeth A, Balkovic J, Ciais P, Deryng D, Folberth C,  
27 758 Glotter M, Hoek S, Iizumi T, Izaurrealde R C, Jones C, Khabarov N, Lawrence P, Liu W, Olin S,  
28 759 Pugh T A M, Ray D K, Reddy A, Rosenzweig C, Ruane A C, Sakurai G, Schmid E, Skalsky R,  
29 760 Song C X, Wang X, De Wit A and Yang H 2017 Global gridded crop model evaluation:  
30 761 Benchmarking, skills, deficiencies and implications *Geosci. Model Dev.* **10** 1403–22
- 31 762 Müller C, Elliott J, Pugh T A M, Ruane A C, Ciais P, Balkovic J, Deryng D, Folberth C, Izaurrealde R  
32 763 C, Jones C D, Khabarov N, Lawrence P, Liu W, Reddy A D, Schmid E and Wang X 2018 Global  
33 764 patterns of crop yield stability under additional nutrient and water inputs *PLoS One* **13** e0198748  
34 765 Online: <https://doi.org/10.1371/journal.pone.0198748>
- 35 766 Müller C, Franke J, Jägermeyr J, Ruane A C, Elliott J, Moyer E, Heinke J, Falloon P, Folberth C,  
36 767 Francois L, Hank T, Izaurrealde R C, Jacquemin I, Liu W, Olin S, Pugh T, Williams K E and  
37 768 Zabel F 2021 Exploring uncertainties in global crop yield projections in a large ensemble of crop  
38 769 models and CMIP5 and CMIP6 climate scenarios *Environ. Res. Lett.*
- 39 770 Olmstead A L and Rhode P W 2011 Adapting North American wheat production to climatic  
40 771 challenges, 1839–2009 *Proc. Natl. Acad. Sci.* **108** 480–5 Online:  
41 772 <http://www.pnas.org/cgi/doi/10.1073/pnas.1008279108>
- 42 773 Osborne T M and Wheeler T R 2013 Evidence for a climate signal in trends of global crop yield  
43 774 variability over the past 50 years *Environ. Res. Lett.* **8**
- 44 775 Ostberg S, Schewe J, Childers K and Frieler K 2018 Changes in crop yields and their variability at  
45 776 different levels of global warming *Earth Syst. Dyn.* **9** 479–96
- 46 777 Oyebamiji O K, Edwards N R, Holden P B, Garthwaite P H, Schaphoff S and Gerten D 2015

- 1  
2  
3 778 Emulating global climate change impacts on crop yields *Stat. Modelling* **15** 499–525
- 4 779 Parkes B, Defrance D, Sultan B, Ciais P and Wang X 2018 Projected changes in crop yield mean and  
5 780 variability over West Africa in a world 1.5K warmer than the pre-industrial era *Earth Syst. Dyn.*  
6 781 **9** 119–34
- 7  
8 782 Peng B, Guan K, Pan M and Li Y 2018 Benefits of Seasonal Climate Prediction and Satellite Data for  
9 783 Forecasting U.S. Maize Yield *Geophys. Res. Lett.* **45** 9662–71 Online:  
10 784 <https://doi.org/10.1029/2018GL079291>
- 11 785 Portmann F T, Siebert S and Döll P 2010 MIRCA2000—Global monthly irrigated and rainfed crop  
12 786 areas around the year 2000: A new high-resolution data set for agricultural and hydrological  
13 787 modeling *Global Biogeochem. Cycles* **24** Online: <https://doi.org/10.1029/2008GB003435>
- 14 788 Raimondo M, Nazzaro C, Marotta G and Caracciolo F 2020 Land degradation and climate change:  
15 789 Global impact on wheat yields *L. Degrad. Dev.*
- 16 790 Ray D K, Gerber J S, Macdonald G K and West P C 2015 Climate variation explains a third of global  
17 791 crop yield variability *Nat. Commun.* **6** 1–9 Online: <http://dx.doi.org/10.1038/ncomms6989>
- 18 792 Ringeval B, Müller C, Pugh T, Mueller N, Ciais P, Folberth C, Liu W, Debaeke P and Pellerin S 2020  
19 793 Potential yield simulated by Global Gridded Crop Models: a process-based emulator to explain  
20 794 their differences *Geosci. Model Dev. Discuss.* 1–39
- 21 795 Rosenzweig C, Elliott J, Deryng D, Ruane A C, Müller C, Arneth A, Boote K J, Folberth C, Glotter M,  
22 796 Khabarov N, Neumann K, Piontek F, Pugh T A M, Schmid E, Stehfest E, Yang H and Jones J W  
23 797 2014 Assessing agricultural risks of climate change in the 21st century in a global gridded crop  
24 798 model intercomparison *Proc. Natl. Acad. Sci.* **111** 3268–73 Online:  
25 799 <http://www.pnas.org/lookup/doi/10.1073/pnas.1222463110>
- 26 800 Rötter R P, Appiah M, Fichtler E, Kersebaum K C, Trnka M and Hoffmann M P 2018 Linking  
27 801 modelling and experimentation to better capture crop impacts of agroclimatic extremes—A  
28 802 review *F. Crop. Res.* **221** 142–56
- 29 803 Ruane A C, Goldberg R and Chryssanthacopoulos J 2015 Climate forcing datasets for agricultural  
30 804 modeling: Merged products for gap-filling and historical climate series estimation *Agric. For.*  
31 805 *Meteorol.* **200** 233–48 Online: <http://dx.doi.org/10.1016/j.agrformet.2014.09.016>
- 32 806 Sacks W J, Deryng D, Foley J A and Ramankutty N 2010 Crop planting dates: an analysis of global  
33 807 patterns *Glob. Ecol. Biogeogr.* **19** 607–20 Online: [https://doi.org/10.1111/j.1466-](https://doi.org/10.1111/j.1466-8238.2010.00551.x)  
34 808 [8238.2010.00551.x](https://doi.org/10.1111/j.1466-8238.2010.00551.x)
- 35 809 Schewe J, Gosling S N, Reyer C, Zhao F, Ciais P, Elliott J, Francois L, Huber V, Lotze H K,  
36 810 Seneviratne S I, van Vliet M T H, Vautard R, Wada Y, Breuer L, Büchner M, Carozza D A,  
37 811 Chang J, Coll M, Deryng D, de Wit A, Eddy T D, Folberth C, Frieler K, Friend A D, Gerten D,  
38 812 Gudmundsson L, Hanasaki N, Ito A, Khabarov N, Kim H, Lawrence P, Morfopoulos C, Müller  
39 813 C, Müller Schmied H, Orth R, Ostberg S, Pokhrel Y, Pugh T A M, Sakurai G, Satoh Y, Schmid  
40 814 E, Stacke T, Steenbeek J, Steinkamp J, Tang Q, Tian H, Tittensor D P, Volkholz J, Wang X and  
41 815 Warszawski L 2019 State-of-the-art global models underestimate impacts from climate extremes  
42 816 *Nat. Commun.* **10** 1–14
- 43 817 Schlenker W and Roberts M J 2009 Nonlinear temperature effects indicate severe damages to U.S. crop  
44 818 yields under climate change. *Proc. Natl. Acad. Sci. U. S. A.* **106** 15594–8
- 45 819 Sternberg T 2011 Regional drought has a global impact *Nature* **472** 169–169
- 46 820 Tack J, Barkley A and Hendricks N 2017 Irrigation offsets wheat yield reductions from warming  
47 821 temperatures *Environ. Res. Lett.* **12**

- 1  
2  
3 822 Tao F, Zhang Z, Zhang S and Rötter R P 2016 Variability in crop yields associated with climate  
4 823 anomalies in China over the past three decades *Reg. Environ. Chang.* **16** 1715–23
- 5 824 Thrasher B L 2012 Technical Note: Bias correcting climate model simulated daily temperature  
6 825 extremes with quantile mapping *Hydrol. Earth Syst. Sci. Discuss.* **9** 5515–29
- 7 826 Tigchelaar M, Battisti D S, Naylor R L and Ray D K 2018 Future warming increases probability of  
8 827 globally synchronized maize production shocks *Proc. Natl. Acad. Sci.* **115** 6644–9
- 9 828 Toreti A, Deryng D, Tubiello F N, Müller C, Kimball B A, Moser G, Boote K, Asseng S, Pugh T A M,  
10 829 Vanuytrecht E, Pleijel H, Webber H, Durand J L, Dentener F, Ceglar A, Wang X, Badeck F,  
11 830 Lecerf R, Wall G W, van den Berg M, Hoegy P, Lopez-Lozano R, Zampieri M, Galmarini S,  
12 831 O’Leary G J, Manderscheid R, Mencos Contreras E and Rosenzweig C 2020 Narrowing  
13 832 uncertainties in the effects of elevated CO<sub>2</sub> on crops *Nat. Food* **1** 775–82 Online:  
14 833 <http://dx.doi.org/10.1038/s43016-020-00195-4>
- 15 834 Trnka M, Rötter R P, Ruiz-Ramos M, Kersebaum K C, Olesen J E, Žalud Z and Semenov M A 2014  
16 835 Adverse weather conditions for European wheat production will become more frequent with  
17 836 climate change *Nat. Clim. Chang.* **4** 637–43
- 18 837 Tubiello F N, Rosenzweig C, Goldberg R A and Jagtap S 2002 Effects of climate change on US crop  
19 838 production: simulation results using two different GCM scenarios. Part I: Wheat, potato, maize,  
20 839 and citrus *Clim. Res.* **20** 259–70 Online: <http://www.int-res.com/abstracts/cr/v20/n3/p259-270/>
- 21 840 Urban D, Roberts M J, Schlenker W and Lobell D B 2012 Projected temperature changes indicate  
22 841 significant increase in interannual variability of U.S. maize yields: A Letter *Clim. Change* **112**  
23 842 525–33
- 24 843 Urban D W, Sheffield J and Lobell D B 2015 The impacts of future climate and carbon dioxide  
25 844 changes on the average and variability of US maize yields under two emission scenarios *Environ.*  
26 845 *Res. Lett.* **10**
- 27 846 Webber H, Ewert F, Olesen J E, Müller C, Fronzek S, Ruane A C, Bourgault M, Martre P, Ababaei B,  
28 847 Bindi M, Ferrise R, Finger R, Fodor N, Gabaldón-Leal C, Gaiser T, Jabloun M, Kersebaum K C,  
29 848 Lizaso J I, Lorite I J, Manceau L, Moriondo M, Nendel C, Rodríguez A, Ruiz-Ramos M,  
30 849 Semenov M A, Siebert S, Stella T, Stratonovitch P, Trombi G and Wallach D 2018 Diverging  
31 850 importance of drought stress for maize and winter wheat in Europe *Nat. Commun.* **9** 1–10 Online:  
32 851 <http://dx.doi.org/10.1038/s41467-018-06525-2>
- 33 852 Wheeler T and Von Braun J 2013 Climate change impacts on global food security *Science (80-. ).* **341**  
34 853 508–13
- 35 854 Wollenberg E, Vermeulen S J, Girvetz E, Loboguerrero A M and Ramirez-Villegas J 2016 Reducing  
36 855 risks to food security from climate change *Glob. Food Sec.* **11** 34–43
- 37 856 Xiong W, Asseng S, Hoogenboom G, Hernandez-Ochoa I, Robertson R, Sonder K, Pequeno D,  
38 857 Reynolds M and Gerard B 2020 Different uncertainty distribution between high and low latitudes  
39 858 in modelling warming impacts on wheat *Nat. Food* **1** 63–9 Online:  
40 859 <http://dx.doi.org/10.1038/s43016-019-0004-2>
- 41 860 Ye Z, Qiu X, Chen J, Cammarano D, Ge Z, Ruane A C, Liu L, Tang L, Cao W, Liu B and Zhu Y 2020  
42 861 Impacts of 1.5 °C and 2.0 °C global warming above pre-industrial on potential winter wheat  
43 862 production of China *Eur. J. Agron.* **120**
- 44 863 You L, Wood S, Wood-Sichra U and Wu W 2014 Generating global crop distribution maps: From  
45 864 census to grid *Agric. Syst.* **127** 53–60 Online: <http://dx.doi.org/10.1016/j.agry.2014.01.002>
- 46 865 Yue Y, Zhang P and Shang Y 2019 The potential global distribution and dynamics of wheat under

- 1  
2  
3 866 multiple climate change scenarios *Sci. Total Environ.* **688** 1308–18 Online:  
4 867 <http://www.sciencedirect.com/science/article/pii/S004896971932724X>  
5 868 Zabel F, Müller C, Elliott J, Minoli S, Jägermeyr J, Schneider J M, Franke J A, Moyer E, Dury M,  
6 869 Francois L, Folberth C, Liu W, Pugh T A M, Olin S, Rabin S S, Mauser W, Hank T, Ruane A C  
7 870 and Asseng S 2021 Large potential for crop production adaptation depends on available future  
8 871 varieties *Glob. Chang. Biol.* 1–13  
9  
10 872 Zaveri E and B. Lobell D 2019 The role of irrigation in changing wheat yields and heat sensitivity in  
11 873 India *Nat. Commun.* **10**  
12  
13 874 Zhao J, Han T, Wang C, Jia H, Worqlul A W, Norelli N, Zeng Z and Chu Q 2020 Optimizing irrigation  
14 875 strategies to synchronously improve the yield and water productivity of winter wheat under  
15 876 interannual precipitation variability in the North China Plain *Agric. Water Manag.* **240** 106298  
16 877 Online: <https://doi.org/10.1016/j.agwat.2020.106298>  
17  
18 878 Zhu P, Zhuang Q, Archontoulis S V., Bernacchi C and Müller C 2019 Dissecting the nonlinear  
19 879 response of maize yield to high temperature stress with model-data integration *Glob. Chang.*  
20 880 *Biol.* **25** 2470–84  
21 881